Preclinical and 'near-patient' models for the evaluation of experimental therapy in prostate and bladder cancer

Merbel, A.F. van de

4 Cationic Amphiphilic Drugs as Potential Anti-Cancer Therapy for Bladder Cancer

Geertje van der Horst
Arjanneke F. van de Merbel
Eline Ruigrok
Maaike H. van der Mark
Emily Ploeg
Laura Appelman
Siri Tvingsholm
Marja Jäätelä
Janneke van Uhm
Marianna Kruithof-de Julio
George N. Thalmann
Rob C.M. Pelger
Chris H. Bangma
Joost L. Boormans
Gabri van der Pluijm
Ellen C. Zwarthoff

Molecular Oncology (2020)

Abstract

More effective therapy for patients with either muscle-invasive or high-risk non-muscle invasive urothelial carcinoma of the bladder (UCB) is an unmet clinical need. For this, drug repositioning of clinically-approved drugs represents an interesting approach. By repurposing existing drugs, alternative anti-cancer therapies can be introduced in the clinic relatively fast, because the safety and dosing of these clinically-approved pharmacological agents are generally well known. Cationic amphiphilic drugs (CADs) dose-dependently decreased the viability of a panel of human UCB lines in vitro. CADs induced lysosomal puncta formation, a hallmark of lysosomal leakage. Intravesical instillation of the CAD penfluridol in an orthotopic mouse xenograft model of human UCB resulted in significantly reduced intravesical tumor growth and metastatic progression. Furthermore, treatment of patient-derived ex-vivo cultured human UCB tissue caused significant partial or complete anti-tumor responses in 97% of the explanted tumor tissues. In conclusion, penfluridol represents a promising treatment option for bladder cancer patients and warrants further clinical evaluation.

Introduction

Urothelial carcinoma of the bladder (UCB) is the fifth most common cancer in the Western world (1). Despite the prevalence and high economic costs of UCB, this cancer is still relatively understudied (2). UCB presents either as non-muscle-invasive (NMIBC) or muscle-invasive carcinoma (MIBC), and many histopathological and molecular subgroups have been defined (3). NMIBC patients undergo transurethral resection of the bladder tumor (TURBT), followed by adjuvant intravesical instillations with Bacillus Calmette-Guérin (BCG) in patients at high risk of recurrence and progression. However, patients do not always tolerate BCG and the risk of relapse in BCG-treated patients varies between 30-40% (4). Neoadjuvant cisplatin-based chemotherapy and radical surgery is the recommended treatment option in non-metastatic MIBC patients. Nevertheless, the 5-year survival rate is only a mere 50% (5). For patients with metastatic UCB, systemic cisplatin-based chemotherapy is the standard of care (6). Taken together, more effective therapies for high-risk NMIBC and advanced or metastatic UCB patients are warranted.

By repurposing existing drugs, alternative anti-cancer therapies can be introduced in the clinic relatively fast, because the safety and dosing of these clinically-approved pharmacological agents are generally well known. The risk of clinical failure due to (serious) adverse effects or reactions, therefore, strongly reduced (7). Consequently, the time needed for bringing the drug from bench-to-bedside is reduced (8). Upon meta-analysis, the overall risk-ratio of cancer incidence was reduced amongst schizophrenia patients, although findings remain controversial (9, 10). Strikingly, the incidence of UCB in patients with schizophrenia is significantly reduced when adjusted for differences in smoking prevalence (9). Strikingly, a class of commonly used antidepressants, antihistamines and antipsychotics- the so-called Cationic Amphiphilic Drugs (CADs)- were previously found to preferentially induce cell death in transformed cells (11). The most potent CADs, including penfluridol, display preferential cytotoxicity towards transformed cells in vitro and potent anti-tumor activity even as single agents in murine tumor models (amongst others in breast, colon, pancreatic and lung carcinoma (11-17).

We hypothesized that CADs display anti-tumor activity in human UCB. We evaluated and compared the potential anti-tumor efficacy of multiple CADs in human UCB cell cultures in vitro, in a preclinical orthotopic human UCB growth and progression model, and in cultured, patient-derived UCB tissue ex-vivo.

Materials and Methods

In vitro
Human UCB cell lines were cultured as described in **Supplementary table 1** (18, 19).

Viability
Cells were seeded as described previously (19). Cells were seeded to reach subconfluency after 24h and subsequently treated for 2h with a dose-range. After replacing the medium, cells were incubated at 37°C for an additional 24, 48 or 72h.

Live cell count
Cell death was measured after 15 min propidium iodide (dead cells;0.2 µg/mL) and Hoechst-33342 staining (live cells;2.5µg/mL) at 37 °C employing Celígo® Cytometer according to the manufacturer's manual.

Apoptosis and Necrosis
Cells were seeded in a 96-wells plate at a density of 10,000 single-cells per well with 3 technical replicates. After 24h, detection reagent (RealTime-Glo™ Assay) was added. Subsequently, a dose-range of penfluridol was added and luminescence and fluorescence were measured using SpectraMax iD3.

Clonogenicity
Clonogenic assay was performed as described previously (19).

Lysosomal membrane permeabilization
60,000 cells were seeded on PET-coated chamber slides and left for 24h to adhere. Cells were treated with a dose-range of penfluridol for 2h. After 24h, lysosomal membrane permeabilization was detected by staining paraformaldehyde-fixed cells with LGALS1 and LAMP-1 (**Supplementary table 1**). Confocal images were taken with TCS_SP8.

Orthotopic in vivo xenograft model
Female BALB/c nude mice (8-weeks old) were housed in ventilated cages under sterile conditions according to Dutch guidelines (evaluated by the Leiden Ethical Animal Welfare committee; DEC_14212; **Supplementary table 1**). Human luciferase-expressing UM-UC3-luc2 cells were inoculated into the bladder as described previously (18) (**Supplementary information**).

For both inoculation of healthy mice and the xenograft model, mice were intravesically treated weekly with either vehicle or penfluridol solution (100μM equivalent to 130 μg/kg/w). The bladder was emptied by mild abdominal massage. Subsequently, 50 μl solution was inserted via an angiocatheter (24G) and the urethra was closed for 1h using a suture. Thereafter, followed by emptying of the bladder (18). Bioluminescence imaging was performed using the IVIS Lumina (18). Quantification of bioluminescent signals was performed by the Living Image® (Xenogen) software. Values were expressed as RLUs in photons/second. Numbers of metastases per animal were counted by eye from a dorsal and ventral view.

Ex-vivo cultured UCB tissues

Tumor tissues from patients diagnosed with various stages of UCB were obtained during transurethral resection of the bladder upon informed consent (evaluated by the Erasmus Medical Ethical Committee MEC-2014-553). Explanted tumor tissue slices (TS) were sectioned and cultured as previously described (20, 21) (**Supplementary information**).

Scoring and inclusion criteria

Upon fixation, paraffin embedding and sectioning, TS were stained for H&E, apoptosis (c-CASP-3), proliferation (PCNA) and cytokeratins (KRT) (20). Stained sections were scanned with a slide scanner and evaluated with Caseviewer. Immunohistochemical evaluations were based on visual estimations from complete histologic tissue sections. Confocal images were taken from representative regions. Criteria for the inclusion of UCB tissue are 1) diagnosis of UCB in TS is confirmed by the pathology report; 2) majority of directly fixed and/or vehicle-treated TS contain tumor cells; 3) size of obtained material is sufficient to perform at least vehicle and 1 CAD dosage. First, H&E stained TS were scored for overall quality (score 0: good quality; 1: poor tissue integrity and quality in >50% of TS area; 4: tissue completely degraded or fragmented). Then, sections were scored for the presence of apoptosis (c-CASP-3+ tumor cells) and fragmented cytokeratin (loss of cell integrity) (score 0: sporadic; 1: multiple clusters). Finally, TS were scored for presence of PCNA (score 1:<50% of KRT+ cells displayed nuclear PCNA). Total score: cumulative individual scores (**Supplementary figure 4**).

Statistics

Analysis was performed using GraphPad Prism 7.0 and Excel. For in vitro assays, one-way ANOVA and Bonferroni post-hoc test. For in vivo: Mann-Whitney-U tests. For ex-vivo: Chi-squared test for categorical data with more than two categories. *p<0.05;**p<0.01;***p<0.001.

Results

Cationic Amphiphilic drugs (CADs) induce lysosomal-dependent cell death in vitro
To identify CADs that display anti-tumor effects, 8 CADs were selected -at least in part- based on a library screen on lung cancer and on the NCI drugs sensitivity database (22). These CADs were initially tested for their effect on viability of T24 and RT-112 human UCB cells in vitro. The CADs penfluridol, astemizole and terfenadine induced the strongest anti-tumor effects upon short-term exposure, (**Figure 1A-B; Supplementary figure 1A-D)**. Subsequently, short-term exposure to a dose-range of these CADs also led to a dose-dependent inhibition in viability of a panel of UCB cells (**Figure 1C-E; Supplementary figure 1E-G**). Viability was decreased when a confluent layer of UCB cells was exposed to a dose-range of penfluridol (**Supplementary figure 1H**). Furthermore, penfluridol significantly decreased the clonogenicity of multiple UCB cell lines (**Figure 1F-G; Supplementary figure 2A-D**). Since we observed strongest anti-tumor potential with penfluridol this compound was used in other disease models in vivo and ex-vivo. Penfluridol treatment resulted in redistribution of phosphatidylserine from the internal to external membrane surface, an early indicator of apoptosis. This was followed by lysis of the cell as measured with a DNA binding dye (**Figure 2A-B**). For the higher dosage (100 μM), only a small increase in apoptosis was observed, and already loss of membrane integrity was observed within 2 hrs. Furthermore, lysosomal LGALS1 puncta formation, a hallmark of lysosomal leakage, was found in penfluridol treated cells (**Figure 2C**) (11, 12, 23, 24).

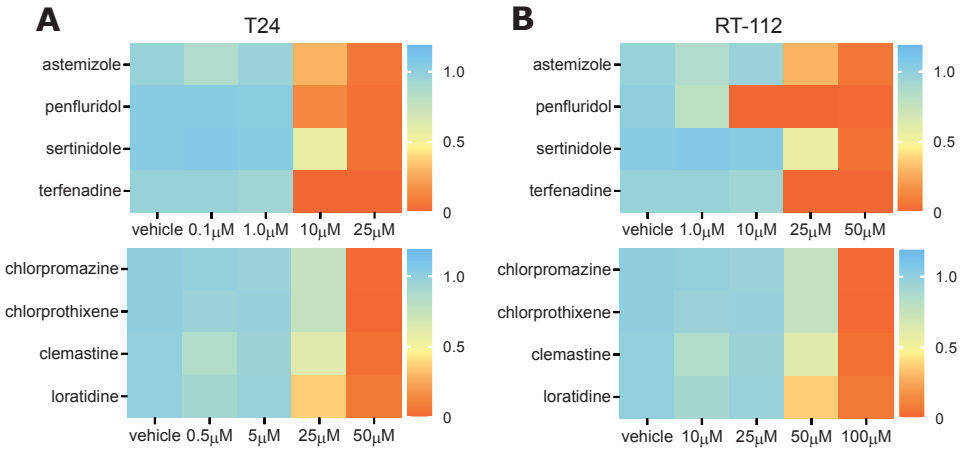

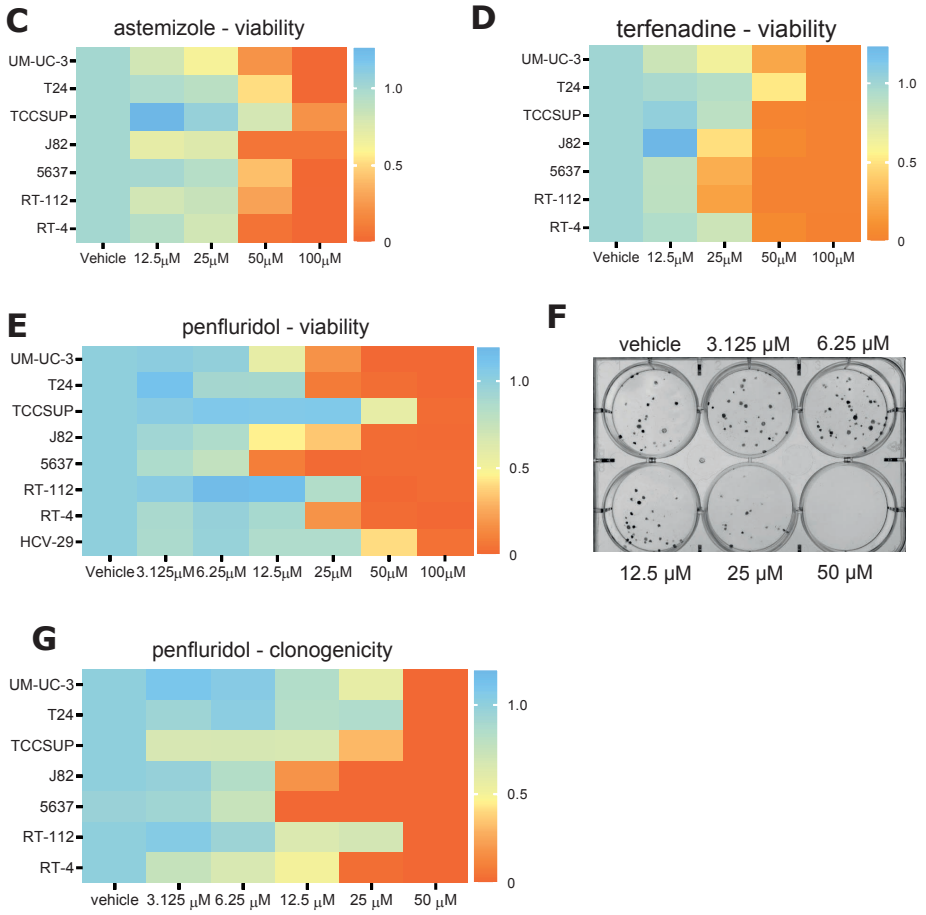

Figure 1 CADs reduce viability and clonogenicity in a panel of human bladder cancer cells.

*Assessment of the viability of T24 (**A**) and RT-112 (**B**) cells after treatment with 8 different CADs for 40h (n=3; 6 replicates each). Panels (**C-E**) represent dose-response experiments with astemizole, terfenadine and penfluridol respectively on the viability of multiple subconfluent bladder cancer cells. Viability was measured 48h after a 2h treatment. Mean normalized to vehicle treated cells. (n=3; 6 replicates each). Clonogenic assay: multiple bladder cancer cells were treated for 2h with a dose range of penfluridol. (**F**) Representative image of a clonogenic assay UM-UC-3 cells. (**G**) The number of colonies was measured using Image J after 10-14 days of culture. (n=3; 3 replicates each).*

Penfluridol inhibits UCB growth and metastasis in a preclinical orthotopic xenograft model

In order to evaluate the anti-tumor effects of penfluridol in a preclinical xenograft mouse model, firefly luciferase2-expressing human UM-UC-3luc2 cells were inoculated in the bladder of female immunodeficient mice (BALB/c nu/nu) (18). Four days after tumor cell inoculation, tumor burden was assessed by whole-body bioluminescence imaging (BLI) and properly inoculated mice were equally distributed among two groups with similar median tumor burden (**Supplementary figure 3A-B**) (18). At this stage, bladder tumor cells have not yet invaded the muscle layer of the murine bladder. Subsequently the mice were treated by weekly intravesical instillations of penfluridol or vehicle solution. Penfluridol significantly reduced total tumor burden by 63% (**Figure 3A-B**). No significant changes were observed in body weight (**Supplementary figure 3C**). At day 29, mice were sacrificed and size and weight of the bladders of penfluridol-treated mice were diminished compared with vehicle-treated animals (**Supplementary figure 3D-E**). As expected, histological examination revealed large orthotopically-growing tumors in vehicle-treated mice with invasion of the tumors into the surrounding connective tissue and muscle layers (**Figure 3C**). In contrast, in penfluridol-treated mice no tumor invasion into the bladder muscle layer was observed and large necrotic regions in tumor tissues at the luminal side of the bladder were detected (**Figure 3D**). All vehicle-treated mice developed metastatic disease with an average of 6.8 metastases/mouse, while only 33% of the penfluridol-treated animals developed distant metastases with an average 4.3/mouse (**Figure 3E**). Metastases were observed in the lungs, reproductive system, liver, intestinal or mesenteric lymph nodes, pancreas, bone and spleen lymph nodes (**Supplementary figure 3F**). Both the number of metastases/mouse and metastatic tumor burden were significantly decreased in penfluridol-treated mice (**Supplementary figure F-G**).

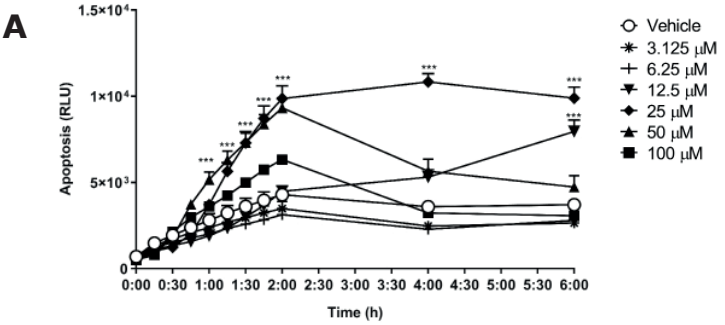
A
Apoptosis (RLU)
1.5×10⁴
1×10⁴
5×10³
0
0:00 0:30 1:00 1:30 2:00 2:30 3:00 3:30 4:00 4:30 5:00 5:30 6:00
Time (h)
Vehicle
3.125 µM
6.25 µM
12.5 µM
25 µM
50 µM
100 µM

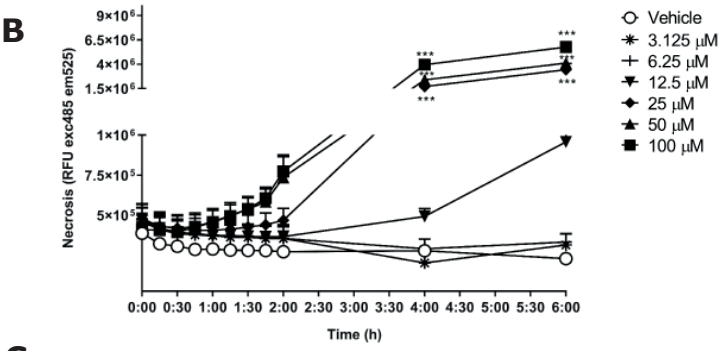
B
Necrosis (RFU exc485 em525)
9×10⁶
6.5×10⁶
4×10⁶
1.5×10⁶
1×10⁶
7.5×10⁵
5×10⁵
0:00 0:30 1:00 1:30 2:00 2:30 3:00 3:30 4:00 4:30 5:00 5:30 6:00
Time (h)
Vehicle
3.125 µM
6.25 µM
12.5 µM
25 µM
50 µM
100 µM

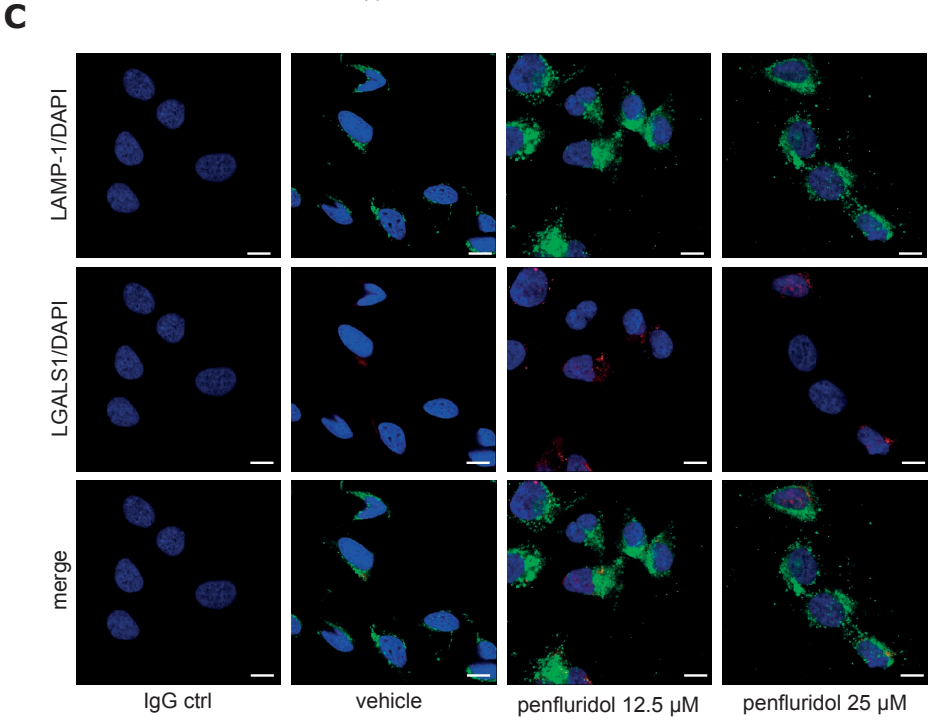
C
LAMP-1/DAPI
LGALS1/DAPI
merge
IgG ctrl
vehicle
penfluridol 12.5 µM
penfluridol 25 µM

◄ Figure 2 Penfluridol induces cell death in human bladder cancer cells.

*(**A**) Real-time apoptosis (luminescence measurement of phosphatidylserine on outer leaflet of cell membranes with Annexin V) and (**B**) cell death (fluorescence measurement of a DNA binding dye) after administration of a dose range of penfluridol. Data presented are mean +/- SE. (n=3; 6 replicates each). One-way ANOVA. *p<0.05; **p<0.01; ***p<0.001. (**C**) Penfluridol targets lysosomal structures in UM-UC-3 cells (n=3, 3 replicates each). Representative images of LAMP-1 (green) LGALS1 (red)/ DAPI (blue) stained UM-UC-3 cells treated for 2h with a dose range of penfluridol.*

Anti-neoplastic response of Penfluridol in ex-vivo cultured, patient-derived cancer tissue slices

Next, we examined the anti-neoplastic effect of penfluridol in our 'near-patient' model, i.e. ex-vivo cultured patient-derived UCB tissue slices (20). Tumor tissues from 57 patients diagnosed with different stages of bladder carcinoma were obtained during transurethral resection of the bladder (TURB) procedures. Tumor tissues from 39/57 patients (68%) were included according to a pre-defined set of tissue quality criteria (see **Materials and methods section 2.3.1**; **Table 1**). Tumor tissues were treated with vehicle solution or a dose-range of penfluridol (n=18) for 3 days. When tumor biopsy material was limited (n=21), explanted tumor tissues were cultured in presence of vehicle solution or 100 µM penfluridol for 3 days. Culturing of the tumor tissue slices under control conditions only marginally affected tissue integrity and viability or not at all, as indicated by marginal differences in immunohistochemical localization of fragmented cytokeratin (indicative of cancer cell debris), apoptotic cells (c-CASP-3) and proliferating cells (PCNA) compared to directly fixed tissue (scoring method in **Supplementary figure 4** and results in **Supplementary figure 5**).

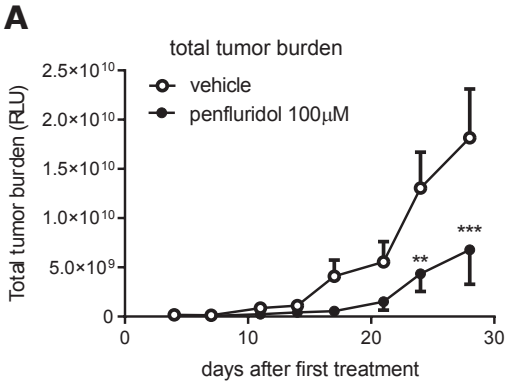

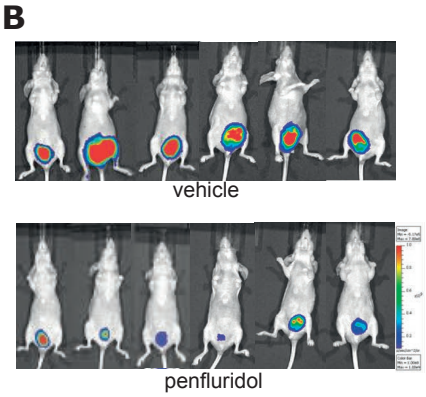

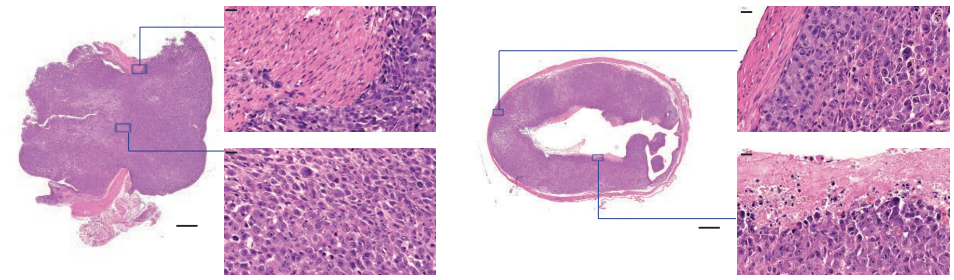

E

% of mice with metastasis in	vehicle	penfluridol
Liver	37.5 %	0 %
Lungs	37.5 %	11%
Reproductive system	62.5 %	11%
Intestinal lymph nodes	75%	22%
Spleen lymph nodes	25%	0 %
Pancreas	12.5%	11%
Bone	12.5%	0 %

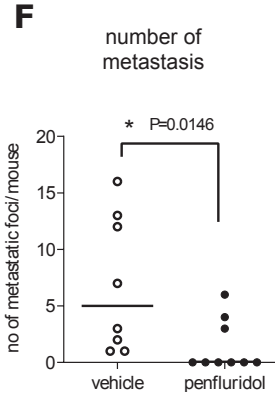

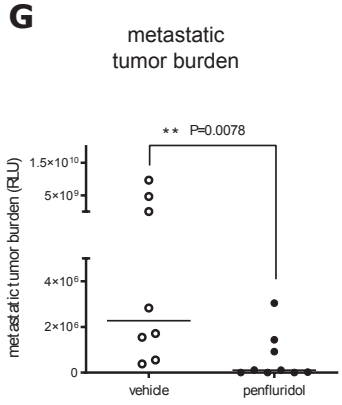

◄ Figure 3 The anti-tumor effects of penfluridol in an orthotopic murine xenograft model with stable firefly luciferase-2 UM-UC-3 human bladder cancer cells.

*Female BALB/c nu/nu mice were inoculated with firefly luciferase2 labelled UM-UC-3 bladder cancer cells and intravesically treated with vehicle (n=8) or penfluridol (n=9); 100 µM once weekly; equivalent to 130 µg/kg/w). (**A**) quantification of the whole-body total tumor burden in real time (relative light units (RLU). Data are presented as mean +/- SE). Mann-Whitney-U test. *p<0.05; **p<0.01; ***p<0.001. (**B**) representative bioluminescent images of vehicle and penfluridol treated mice at day 29. Representative images of vehicle (**C**) and penfluridol (**D**) treated bladders stained with Hematoxylin & Eosin. Scale bar 500 and 20 µm respectively. (**E**) The percentage of mice with detectable metastases in the listed organs. (**F**) number of metastatic foci per mouse per experimental group. (**G**) metastatic tumor burden per experimental group (RLU). Mann-Whitney-U test. *p<0.05; **p<0.01; ***p<0.001.*

In almost all patients (35/39), strong changes were observed after treatment with penfluridol, ranging from complete loss of tumor to significant reduction of the tumor (**Figure 4A**). An overall reduction in the number of UCB cells, proliferating cells (PCNA), increased numbers of apoptotic cells (c-CASP-3) and significantly increased amounts of fragmented cytokeratins were observed (P value=4,36424E-11, X2 test). In tissue slices obtained from only three patients, partial anti-neoplastic responses were registered (e.g. an induction of apoptosis). In tissue slices obtained from one patient (1/39), no response to the treatment was found. The effect of a dose-range of penfluridol revealed that, starting from 12.5 µM, major anti-neoplastic changes were observed (**Figure 4C-D**).

► **Table 1 Patient characteristics.**

Tumor tissues from 57 patients diagnosed with various stages of urothelial carcinoma of the bladder were obtained during transurethral resection of the bladder (TURBT upon informed consent, MEC-2014-553). Tumor tissues from 39 patients were included according to the tissue quality inclusion criteria. Disease stage, grade, presence of CIS and detrusor was determined by a pathologist. Patient #40 is a patient diagnosed with prostate carcinoma Gleason grade 3+4 with no history of UCB. NA: not applicable. BCG: Bacillus Calmette-Guérin.

patient no	stage	grade	tumor	recurrence frequency	cis present	detrusor present	previous treatment	previous treatment modality	gender	age
1	Ta	G1	primary	NA	unknown	yes	no	NA	male	75
2	Ta	G1	primary	NA	unknown	yes	no	NA	male	71
3	Ta	G1	recurrence	>1 / year	unknown	yes	unknown	unknown	male	72
4	Ta	G1	primary	NA	unknown	yes	no	NA	female	69
5	Ta	G1	primary	NA	unknown	no	no	NA	male	62
6	Ta	G1	recurrence	>1 /year	unknown	no	yes	nephroureterectomies	male	63
7	Ta	G2	primary	NA	unknown	yes	no	NA	male	76
8	Ta	G2	primary	NA	no	yes	no	NA	male	67
9	Ta	G2	recurrence	>1 /year	no	yes	yes	TURBT	male	86
10	Ta	G2	recurrence	>1 /year	no	yes	yes	chemotherapy	male	56
11	Ta	G2	recurrence	>1 /year	no	yes	yes	BCG	male	87
12	Ta	G2	recurrence	>1 /year	no	yes	yes	nephroureterectomies	male	62
13	Ta	G2	primary	NA	no	unknown	no	NA	male	39
14	Ta	G2	recurrence	>1 /year	no	yes	yes	BCG	male	59
15	Ta	G2	primary	NA	no	yes	no	NA	female	69
16	Ta	G2	recurrence	>1 /year	no	yes	yes	chemotherapy	female	53
17	Ta	G2	recurrence	>1 /year	no	yes	yes	Chemohyperthermia	male	57
18	Ta	G2	primary	NA	no	yes	no	NA	male	79
19	Ta	G2	primary	NA	no	yes	no	NA	male	73
20	Ta	G2	recurrence	<1 / year	no	yes	yes	chemotherapy	male	75

► **Table 1 Patient characteristics Contiuned.**

patient no	stage	grade	tumor	recurrence frequency	cis present	detrusor present	previous treatment	previous treatment modality	gender	age
21	Ta	G2	recurrence	>1 /year	no	yes	yes	BCG	female	59
22	Ta	G2	recurrence	unknown	no	yes	yes	chemoradiation	male	84
23	Ta	G3	primary	NA	no	yes	no	NA	male	75
24	Ta	G3	recurrence	>1 /year	no	no	yes	BCG	male	76
25	Ta	G3	primary	NA	unknown	no	no	NA	male	56
26	Ta	unknown	primary	<1 / year	no	unknown	no	NA	female	53
27	T1	G2	recurrence	<1 / year	unknown	no	no	NA	male	86
28	T1	G2	recurrence	>1 /year	no	yes	yes	BCG	male	74
29	T1	G2	primary	NA	yes	yes	no	NA	male	67
30	T1	G2	primary	NA	no	yes	no	NA	male	55
31	T1	G3	primary	NA	no	yes	yes	TURBT	male	66
32	T1	G3	recurrence	>1 /year	no	yes	yes	BCG	male	52
33	T1	G3	primary	NA	no	no	no	NA	female	67
34	T1	G3	primary	NA	unknown	yes	no	NA	male	81
35	T2	G3	primary	NA	no	yes	no	NA	male	74
36	T2	G3	primary	NA	yes	yes	no	NA	male	58
37	T2	G3	recurrence	>1 /year	yes	yes	no	NA	male	72
38	T2	G3	primary	NA	unknown	yes	no	NA	male	66
39	T2	highgrade	primary	NA	unknown	yes	no	NA	male	64
40	T3	Gl3+4	primary	NA	NA	NA	yes	LHRH agonist	male	65

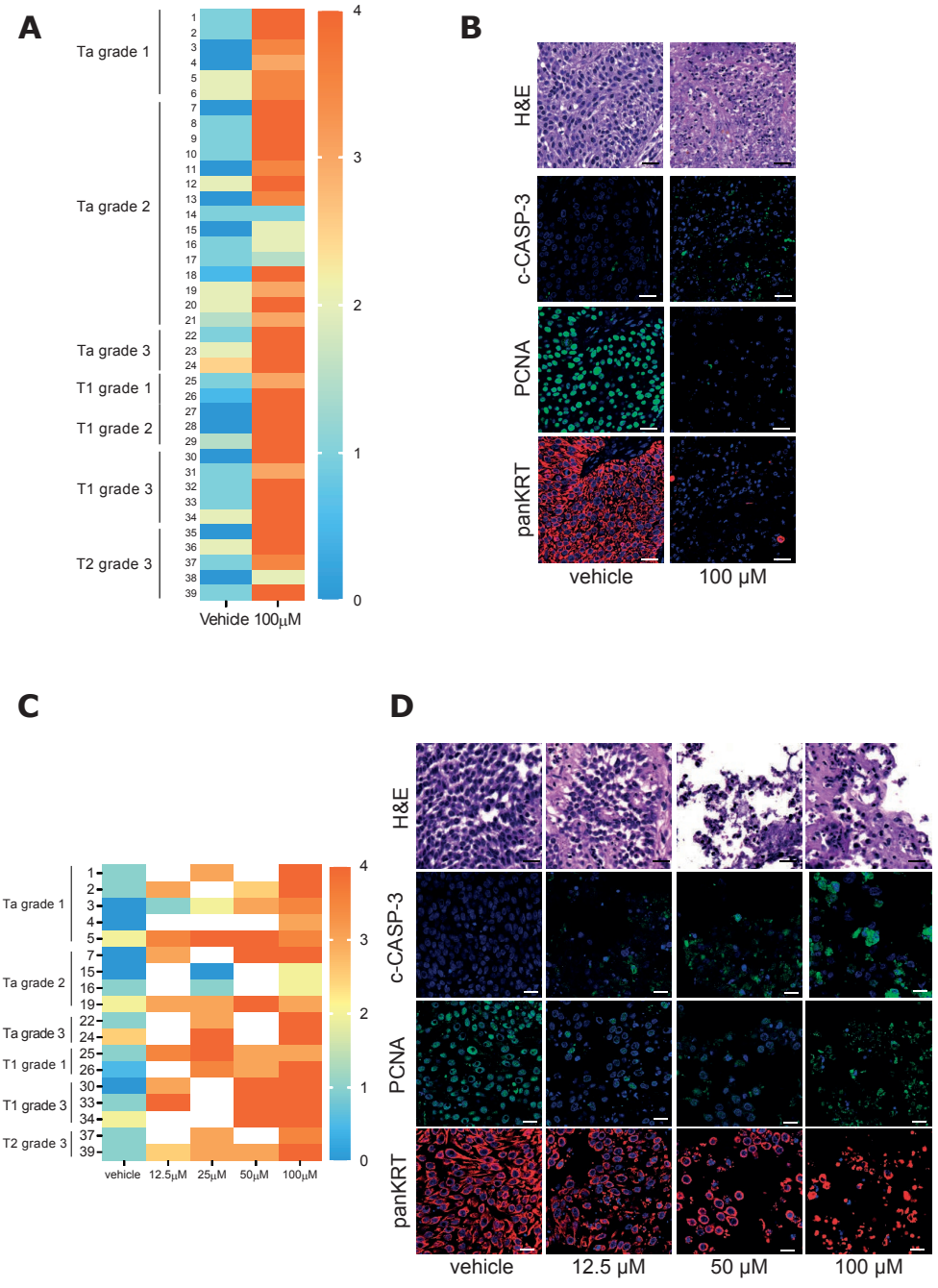
A
Ta grade 1
Ta grade 2
Ta grade 3
T1 grade 1
T1 grade 2
T1 grade 3
T2 grade 3
Vehide 100μM
B
H&E
c-CASP-3
PCNA
panKRT
vehicle
100 μM
C
Ta grade 1
Ta grade 2
Ta grade 3
T1 grade 1
T1 grade 3
T2 grade 3
vehicle
12.5μM
25μM
50μM
100μM
D
H&E
c-CASP-3
PCNA
panKRT
vehicle
12.5 μM
50 μM
100 μM

◄ Figure 4 Ex-vivo treatment of cultured human bladder cancer slices with penfluridol.
*Heat maps showing median cumulative scores of the bladder cancer slices per condition per patient. Multiple explanted tissue slices were cultured for each condition. Cumulative score is based on histological evaluation of entire tissue slice (TS; see **Supplementary figure 4**). TS were scored in 4 categories: 1) overall quality based on H&E staining, 2) presence of apoptotic cells (cleaved-caspase 3+(c-CASP-3+)/ Keratin+ (KRT+) cells) and 3) cancer cell debris (fragmented Keratin), and 4) nuclear proliferation based on proliferation cell nuclear antigen (PCNA). TS received a score of either 0 or 1 for each category. For category 1, TS received a score of 1 for >50% of tissue was fragmented/degraded. For category 2 and 3, TS received a score of 1 when multiple clusters were observed. For category 4, TS received a score of 1 when <50% of KRT+ cells in the TS displayed nuclear PCNA. Cumulative score was calculated as the sum of the 4 categories, median cumulative scores are shown. (see also **Supplementary figure 4**) Explanted tumor slices were ex-vivo cultured with vehicle solution or penfluridol (100 μM for **A-B** and a dose range for **C-D**) for 3 days. Chi-squared test for categorical data with more than two categories. P value=4,36424E-11. (**B**) Representative images of bladder cancer slices obtained from a patient diagnosed with NMIBC stage T1 grade 2 (#28) after 3 days in the presence of vehicle solution or penfluridol (100 μM). Complete loss of tumor cells was observed in 5 patient-derived tumor explants (#9,28,29,31 and 35). Significant reduction was found in 30 patient-derived tumor explants (#1-8, 10-15, 17, 20, 22-27, 30, 32-34 and 36-39). A partial response was observed in 3 patient-derived tumor explants (#18,19 and 21). No response was observed in one patient-derived tumor explant (#16). (**D**) Representative images of bladder cancer tissue slices obtained from a patient diagnosed with NMIBC stage T1 grade 2 (#9) after 3 days in the presence of vehicle solution or a dose range of penfluridol. c-CASP-3 and PCNA: green, panKRT red and DAPI blue. Scalebar 25 μm.*

Penfluridol has no effect on normal urothelium.

Intravesical treatment represents a potential alternative route of administration of CADs for the treatment of localized bladder cancer. In order to evaluate safety of penfluridol instillations on normal urothelium, a dose-range of penfluridol was administered to non-tumor bearing mice by weekly intravesical treatment (**Figure 5A**). Histological analyses revealed no detectable changes of normal murine urothelium after multiple doses of intravesical penfluridol (**Figure 5B-D**). Moreover, while penfluridol treatment of ex-vivo cultured patient-derived UCB tissues caused significant anti-tumor effects, adjacent 'normal' human urothelium was not or only marginally affected (**Supplementary figure 6A-B**). No changes were observed in epithelial tissue integrity, the proliferation index (PCNA), viable epithelial cell numbers or fragmented KRT, despite a mildly increased apoptotic response (**Supplementary figure 6A**).

Because matched normal urothelium samples are scarce, we assessed the effect of penfluridol on 'normal' urothelium of a prostate cancer patient with no history of bladder carcinoma. Again, no detectable tissue integrity changes were observed in the penfluridol-treated human urothelium versus vehicle treated urothelium. Limited c-CASP-3+ cells were only observed in the penfluridol-treated normal urothelium layers but no detectable changes of urothelium tissue integrity were found (**Figure 5E**).

► Figure 5 Evaluation of the effect of penfluridol on normal murine or human urothelium integrity.

*(**A**) Average body weight (mean +/- SE) of non-tumor bearing female BALB/c nu/nu mice treated intravesically with vehicle (n=5) or penfluridol solution (n=5 ;100 µM once weekly for 4 weeks; equivalent to 130 µg/kg/w). One-way ANOVA. *p<0.05; **p<0.01; ***p<0.001. Representative overview images of H&E stained murine bladders of vehicle-treated (**B**) and 100 µM penfluridol-treated (**C**) mice. (**D**) Representative images of vehicle- and penfluridol-treated, non-tumor bearing murine bladders. c-CASP-3 and PCNA: green, panKRT red and DAPI blue. Scalebar H&E 20 µm, IF staining 25 µm. (**E**) Representative images of non-transformed 'normal' urothelium in tissue slices obtained from a patient with prostate cancer with no history of bladder carcinoma, treated either with vehicle solution or 100 µM penfluridol for 3 days (#40). c-CASP-3 and PCNA: green, panKRT red and DAPI blue. Scalebar 25 µm.*

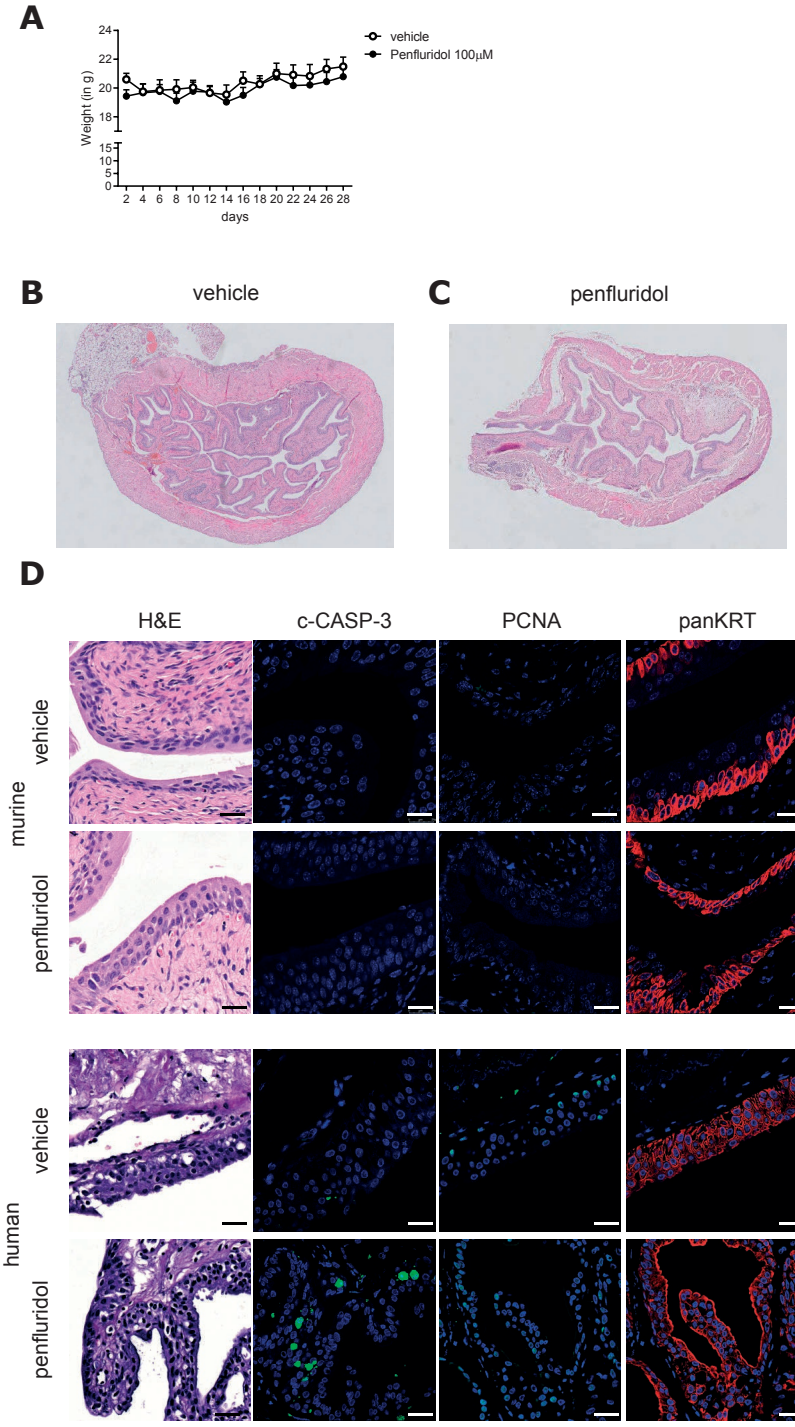
A
vehicle
Penfluridol 100μM
Weight (in g)
days
B
vehicle
C
penfluridol
D
H&E
c-CASP-3
PCNA
panKRT
murine
vehicle
penfluridol
human
vehicle
penfluridol

Discussion

In this study, we provide compelling evidence that CADs display significant anti-tumor effects in multiple preclinical bladder cancer models, i.e. cultured human UCB cells in vitro, an orthotopic preclinical xenograft model of UCB growth and metastasis in vivo, and patient-derived ex-vivo cultured UCB tissues. Screening of eight different CADs in a panel of cultured human UCB cell lines identified penfluridol as a potent candidate anti-cancer agent. We observed that the anti-tumor properties of penfluridol in human UCB may rely on rapid destabilization of lysosomal structures in human UCB cells. Our data in UCB are in line with the observed anti-neoplastic effects of CADs in other solid tumors (11-17). Other anti-neoplastic mechanisms of this class of compounds may also play a role, including anti-migratory and invasion effects, cell cycle effects, changes in cholesterol homeostasis, autophagy, immune modulation or non-homologous end-joining (reviewed in (25-27)).

CADs have been shown to induce lysosome-dependent cell death mediated by lysosomal cathepsin proteases leaking from the destabilized lysosomes to the cytosol in other tumors (28-30). Selectivity of the CADs for transformed cells is due to the lower constitutional acid sphingomyelin levels in their lysosomes compared to healthy cells. CADs reduce ASM levels to the point of lysosomal membrane permeabilization which leads to lysosome-dependent cell death specifically in transformed cells (28, 29, 31). Selectivity of CADs for transformed bladder epithelial cells is further substantiated by the observed lack of adverse effects of CAD treatment on normal urothelium, which was not (or only marginally) affected after intra-vesical administration of a same dose of penfluridol in a non-tumor bearing in vivo model and administration of penfluridol to ex-vivo cultured normal human bladder tissue. In our preclinical disease model of orthotopically growing human UCB, weekly intravesical instillation with penfluridol significantly reduced tumor progression, invasion and formation of distant metastases. Our preclinical data demonstrate that effective delivery of penfluridol can be achieved by instillation in the bladder thus mimicking the clinical use of standard-of-care pharmacological agents mitomycin C or BCG. This way potential adverse systemic side effects of this class of antipsychotic drugs may be largely avoided.

For UCB patients that present with a disease confined to the mucosa (stage Ta, CIS) or submucosa (stage T1) treatment consists of transuretheral resection of the bladder (TURB) followed by an immediate postoperative intravesical instillation with chemotherapy. In patients who are at intermediate- or high-risk of recurrence, maintenance treatment with intravesical chemo- or immunotherapy is advocated in the guidelines. In general, chemotherapy with mitomycin C or epirubicin for 1 year (4 weekly instillations followed by 6-8 monthly instillations) is indicated in intermediate-risk patients, whereas high-risk patients are treated with 1 to 3 years of Bacillus Calmette-Guérin (BCG) (32). Patients in whom NMIBC recurs after TURB and BCG treatment, and who have BCG unresponsive disease, are unlikely to respond to further BCG therapy and may need a cystectomy. The alternative treatment option is lifelong cystoscopic surveillance and frequent TURB re-operations are necessary. Obvious downsides of radical cystectomy are that it is a major surgical procedure with substantial cost and a negative impact on the quality of life of patients. If feasible, patients often prefer a bladder sparing treatment and new intravesical therapies are being developed in clinical trials (33).

Despite these new developments, only Valrubucin -a doxorubucin-analog- was FDA-approved for BCG-refractory CIS (34). Based on the growing body of evidence and the previously established safety profile of CADs as FDA-approved drugs, penfluridol appears to be a promising anti-cancer compound, especially when systemic exposure is reduced by intravesical administration to patients with (recurrent) high risk bladder cancer. Taken together, our current findings emphasize the need for a clinical trial that will address safety and anti-tumor efficacy aspects of intravesical penfluridol in organ-confined bladder cancer.

Conclusions

Cationic amphiphilic drugs like penfluridol significantly reduced UCB cell viability. Weekly bladder instillations of penfluridol resulted in significant decreased tumor growth, progression and metastasis in vivo. Treatment of cultured patient-derived UCB tissue slices with penfluridol resulted in significant anti-tumor responses ranging from complete loss of tumor to significant reduction. Normal urothelium, when treated with penfluridol was not at all or only marginally affected upon instillation of CADs in a preclinical UCB in vivo model and cultured normal human bladder tissue slices ex-vivo.

Taken together, penfluridol is a promising anti-cancer agent in human UCB and clinical studies are required to determine if this FDA-approved antipsychotic agent can provide a benefit to patients with UCB.

Financial support

Dutch Cancer Society (KWF) grant Unieke Kansen (EMCR 2015-8038), European Research Council (AdG 340751) and Danish National Research Foundation (DNRF125).

References

1. Ploeg M, Aben KK, Kiemeney LA. The present and future burden of urinary bladder cancer in the world. World journal of urology. 2009;27(3):289-93.

2. Avritscher EB, Cooksley CD, Grossman HB, Sabichi AL, Hamblin L, Dinney CP, et al. Clinical model of lifetime cost of treating bladder cancer and associated complications. Urology. 2006;68(3):549-53.

3. Alifrangis C, McGovern U, Freeman A, Powles T, Linch M. Molecular and histopathology directed therapy for advanced bladder cancer. Nature reviews Urology. 2019.

4. Sylvester RJ, van der MA, Lamm DL. Intravesical bacillus Calmette-Guerin reduces the risk of progression in patients with superficial bladder cancer: a meta-analysis of the published results of randomized clinical trials. J Urol. 2002;168(5):1964-70.

5. Madersbacher S, Hochreiter W, Burkhard F, Thalmann GN, Danuser H, Markwalder R, et al. Radical cystectomy for bladder cancer today--a homogeneous series without neoadjuvant therapy. J Clin Oncol. 2003;21(4):690-6.

6. Alfred Witjes J, Lebret T, Comperat EM, Cowan NC, De Santis M, Bruins HM, et al. Updated 2016 EAU Guidelines on Muscle-invasive and Metastatic Bladder Cancer. Eur Urol. 2017;71(3):462-75.

7. Ashburn TT, Thor KB. Drug repositioning: identifying and developing new uses for existing drugs. Nat Rev Drug Discov. 2004;3(8):673-83.

8. Bhattarai D, Singh S, Jang Y, Hyeon Han S, Lee K, Choi Y. An Insight into Drug Repositioning for the Development of Novel Anti-Cancer Drugs. Current topics in medicinal chemistry. 2016;16(19):2156-68.

9. Catts VS, Catts SV, O'Toole BI, Frost AD. Cancer incidence in patients with schizophrenia and their first-degree relatives - a meta-analysis. Acta psychiatrica Scandinavica. 2008;117(5):323-36.

10. Li H, Li J, Yu X, Zheng H, Sun X, Lu Y, et al. The incidence rate of cancer in patients with schizophrenia: A meta-analysis of cohort studies. Schizophrenia research. 2018;195:519-28.

11. Petersen NH, Olsen OD, Groth-Pedersen L, Ellegaard AM, Bilgin M, Redmer S, et al. Transformation-associated changes in sphingolipid metabolism sensitize cells to lysosomal cell death induced by inhibitors of acid sphingomyelinase. Cancer Cell. 2013;24(3):379-93.

12. Ostenfeld MS, Fehrenbacher N, Hoyer-Hansen M, Thomsen C, Farkas T, Jaattela M. Effective tumor cell death by sigma-2 receptor ligand siramesine involves lysosomal leakage and oxidative stress. Cancer research. 2005;65(19):8975-83.

13. Ranjan A, German N, Mikelis C, Srivenugopal K, Srivastava SK. Penfluridol induces endoplasmic reticulum stress leading to autophagy in pancreatic cancer. Tumor Biol. 2017;39(6).

14. Ranjan A, Gupta P, Srivastava S. Penfluridol suppresses triple negative breast cancer metastasis to brain by inhibiting alpha 6 beta 4 integrins. Cancer research. 2015;75.

15. Ranjan A, Srivastava SK. Repurposing antipsychotic drug Penfluridol for cancer treatment. Cancer research. 2014;74(19).

16. Ranjan A, Srivastava SK. Penfluridol suppresses pancreatic tumor growth by autophagy-mediated apoptosis. Sci Rep-Uk. 2016;6.

17. Ranjan A, Srivastava SK. Penfluridol suppresses glioblastoma tumor growth by Akt-mediated inhibition of GLI1. Oncotarget. 2017;8(20):32960-76.

18. van der Horst G, van Asten JJ, Figdor A, van den Hoogen C, Cheung H, Bevers RF, et al. Real-Time Cancer Cell Tracking by Bioluminescence in a Preclinical Model of Human Bladder Cancer Growth and Metastasis. EurUrol. 2011;%19.

19. van der Horst G, Bos L, van der Mark M, Cheung H, Heckmann B, Clement-Lacroix P, et al. Targeting of alpha-v integrins reduces malignancy of bladder carcinoma. PLoSOne. 2014;9(9):e108464.

20. van de Merbel AF, van der Horst G, van der Mark MH, van Uhm JIM, van Gennep EJ, Kloen P, et al. An ex vivo Tissue Culture Model for the Assessment of Individualized Drug Responses in Prostate and Bladder Cancer. Front Oncol. 2018;8:400.

21. Karkampouna S, Kruithof BP, Kloen P, Obdeijn MC, van der Laan AM, Tanke HJ, et al. Novel Ex Vivo Culture Method for the Study of Dupuytren's Disease: Effects of TGFbeta Type 1 Receptor Modulation by Antisense Oligonucleotides. Molecular therapy Nucleic acids. 2014;3:e142.

22. Ellegaard AM, Dehlendorff C, Vind AC, Anand A, Cederkvist L, Petersen NHT, et al. Repurposing Cationic Amphiphilic Antihistamines for Cancer Treatment. EBioMedicine. 2016;9:130-9.

23. Ellegaard AM, Groth-Pedersen L, Oorschot V, Klumperman J, Kirkegaard T, Nylandsted J, et al. Sunitinib and SU11652 inhibit acid sphingomyelinase, destabilize lysosomes, and inhibit multidrug resistance. Mol Cancer Ther. 2013;12(10):2018-30.

24. Sukhai MA, Prabha S, Hurren R, Rutledge AC, Lee AY, Sriskanthadevan S, et al. Lysosomal disruption preferentially targets acute myeloid leukemia cells and progenitors. The Journal of clinical investigation. 2013;123(1):315-28.

25. Du J, Shang J, Chen F, Zhang Y, Yin N, Xie T, et al. A CRISPR/Cas9-Based Screening for Non-Homologous End Joining Inhibitors Reveals Ouabain and Penfluridol as Radiosensitizers. Mol Cancer Ther. 2018;17(2):419-31.

26. Ranjan A, Gupta P, Srivastava SK. Penfluridol: An Antipsychotic Agent Suppresses Metastatic Tumor Growth in Triple-Negative Breast Cancer by Inhibiting Integrin Signaling Axis. Cancer research. 2016;76(4):877-90.

27. Wu L, Liu YY, Li ZX, Zhao Q, Wang X, Yu Y, et al. Anti-tumor Effects of Penfluridol through Dysregulation of Cholesterol Homeostasis. Asian Pac J Cancer P. 2014;15(1):489-94.

28. Aits S, Jaattela M. Lysosomal cell death at a glance. Journal of cell science. 2013;126(Pt 9):1905-12.

29. Halliwell WH. Cationic amphiphilic drug-induced phospholipidosis. Toxicol Pathol. 1997;25(1):53-60.

30. Towers CG, Thorburn A. Targeting the Lysosome for Cancer Therapy. Cancer Discov. 2017;7(11):1218-20.

31. Barcelo-Coblijn G, Martin ML, de Almeida RF, Noguera-Salva MA, Marcilla-Etxenike A, Guardiola-Serrano F, et al. Sphingomyelin and sphingomyelin synthase (SMS) in the malignant transformation of glioma cells and in 2-hydroxyoleic acid therapy. Proc Natl Acad Sci U S A. 2011;108(49):19569-74.

32. Lamm DL, Blumenstein BA, Crissman JD, Montie JE, Gottesman JE, Lowe BA, et al. Maintenance bacillus Calmette-Guerin immunotherapy for recurrent TA, T1 and carcinoma in situ transitional cell carcinoma of the bladder: a randomized Southwest Oncology Group Study. J Urol. 2000;163(4):1124-9.

33. Tse J, Singla N, Ghandour R, Lotan Y, Margulis V. Current advances in BCG-unresponsive non-muscle invasive bladder cancer. Expert Opin Investig Drugs. 2019;28(9):757-70.

34. Kang M, Jeong CW, Kwak C, Kim HH, Ku JH. Single, mmediate postoperative instillation of chemotherapy in non-muscle invasive bladder cancer: a systematic review and network meta-analysis of randomized clinical trials using different drugs. Oncotarget. 2016;7(29):45479-88.

Supplementary table

► Supplementary table 1 key resources

Key reagents and resources used in the manuscript with their respective suppliers, Research Resource Identifiers (RRID) and additional information. Cells were routinely cultured in a humidified incubator at 37°C and 5% CO2 and were regularly (once every 2 months) tested for mycoplasm by RT-PCR. Supplements were from Life Technologies, Gibco. For used antibodies, respective dilutions were added and the indicated time in the pressure cooker (PC) when antigen retrieval was performed by cooking the slides in unmasking solution (Vector Labs, H-3300); N.A. not applicable.

Supplementary table 1 key resources.

Key reagents and resources used in the manuscript with their respective suppliers, Research Resource Identifiers (RRID) and additional information. Cells were routinely cultured in a humidified incubator at 37°C and 5% CO2 and were regularly (once every 2 months) tested for mycoplasm by RT-PCR. Supplements were from Life Technologies, Gibco. For used antibodies, respective dilutions were added and the indicated time in the pressure cooker (PC) when antigen retrieval was performed by cooking the slides in unmasking solution (Vector Labs, H-3300); N.A. not applicable.

Experimental models: cell lines					
Cell line	**Source**	**Identifier**	**Medium**	**Supplier**	**Supplements**
UM-UC-3	ATCC	ATCC Cat# CRL-1749, RRID:CVCL_1783	Eagle's minimal essential medium (EMEM)	ATCC, 30-2003	10% FBS , 100 units/ ml penicillin, 50 µg/ml streptomycin
J82	ATCC	ATCC Cat# HTB-1, RRID:CVCL_0359	Dulbecco's Modified Eagle medium (DMEM)	Life technologies, Gibco, 31966-021	10% FBS , 100 units/ ml penicillin, 50 µg/ml streptomycin
T24	ATCC	ATCC Cat# HTB-4, RRID:CVC L_0554	RPMI 1640	Lonza, BE12-167F	10% FBS , 100 units/ ml penicillin, 50 µg/ml streptomycin, GLUTAMAX

Supplementary table 1 Continued.

Experimental models: cell lines					
Cell line	**Source**	**Identifier**	**Medium**	**Supplier**	**Supplements**
TCCSUP	ATCC	ATCC Cat# HTB-5, RRID:CVCL_1738	Eagle's minimal essential medium (EMEM)	ATCC, 30-2003	10% FBS , 100 units/ml penicillin, 50 µg/ml streptomycin
RT-112	Cell lines service. https:// clsgmbh.de	CLS Cat# 300324/p10280_ RT-112, RRID:CVCL_1670	Dulbecco's Modified Eagle medium (DMEM)	Life technologies, Gibco, 31966-021	10% FBS , 100 units/ml penicillin, 50 µg/ml streptomycin
5637	ATCC	ATCC Cat# HTB-9, RRID:CVCL_0126	RPMI 1640	Lonza, BE12-167F	10% FBS , 100 units/ml penicillin, 50 µg/ml streptomycin, GLUTAMAX
RT-4	ATCC	ATCC Cat# HTB-2, RRID:CVCL_0036	McCoy's 5A	Thermo Fisher Scientific Invitrogen 36600-021	10% FBS , 100 units/ml penicillin, 50 µg/ml streptomycin, GLUTAMAX

Supplementary table 1 Continued.

Experimental models: organisms and strains					
Cell line	**Source**	**Identifier**	**Gender**	**Ethical committee**	**Ethical protocol**
Female balb c nude mice (CAnN.Cg-Foxn1nu/Crl)	Charles River Laboratories RRID: SCR_003792	RRID: MGI:2160479	Female	Committee on the Ethics of Animal Experiments of Leiden University, The Netherlands	DEC_14212
Experimental models: biological samples					
Biological sample	**Source**	**Identifier**	**Gender**	**Ethical committee**	**Ethical protocol**
Human bladder samples transurethral resection of the bladder (TURB)	Erasmus Medical Center bladder cancer biobank	Coded samples			MEC-2014-553

Supplementary table 1 Continued.

Antibodies				
Antibody	**Source**	**Identifier**	**Dilution**	**PC**
Mouse-anti human Proliferating cell nuclear antigen (PCNA)	Sigma-Aldrich, P8825	RRID: AB_477413	1:2000	40’
Rabbit anti-human Pan cytokeratin (panKRT)	Life technologies, 180059	RRID: AB_10942225	1:250	40’
Guinea Pig anti-murine Pan cytokeratin (panKRT)	Origene, BP5069	RRID: AB_979529	1:250	40’
Goat anti-human Collagen I	Southerenbiotech, 1310-01	RRID: AB_2753206	1:1000	40’
Rabbit anti-human Cleaved caspase-3 (c-CASP-3)	Cell signaling, 9661L	RRID: AB_2341188	1:500	40’
Mouse anti-human Keratin 18 (KRT18)	Dako, M7010	RRID:AB_2133299	1:500	40’
Mouse anti-human LAMP-1	Abcam ab25630	RRID:AB_470708	1:20	N.A.

Supplementary table 1 Continued.

Antibodies				
Antibody	**Source**	**Identifier**	**Dilution**	**PC**
Rabbit anti-human Galectin-1 (LGALS1)	AbCaM ab25138	, RRID:AB_2136615	1:2000	N.A.
Donkey-anti Mouse Alexa Fluor 488	Life technologies, R37114	RRID:AB_2556542	1:250	N.A.
Donkey-anti Rabbit Alexa Fluor 488	Life technologies, A-21206	RRID:AB_141708	1:250	N.A.
Donkey-anti Mouse Alexa Fluor 555	Life technologies, A-31570	RRID:AB_2536180	1:250	N.A.
Donkey-anti Rabbit Alexa Fluor 555	Life technologies, A-31572	RRID:AB_162543	1:250	N.A.
Donkey-anti Goat Alexa Fluor 647	Life technologies, A-31572	RRID:AB_141844	1:250	N.A.
Goat-anti Guinea Pig Alexa Fluor 647	Life technologies, A-21450	RRID:AB_2735091	1:250	N.A.

Supplementary table 1 Continued.

Chemicals		
Chemical	**Source**	**Identifier**
Penfluridol	Sigma-Aldrich RRID:SCR_008988	P3371
Astemizole	Sigma-Aldrich RRID:SCR_008988	A2861
Terfenadine	Sigma-Aldrich RRID:SCR_008988	T9652
Sertinidole	Sigma-Aldrich RRID:SCR_008988	S8072
Chlorprothixene	Sigma-Aldrich RRID:SCR_008988	C1671
Chlorpromazine	Sigma-Aldrich RRID:SCR_008988	C8138
Clemastine	Sigma-Aldrich RRID:SCR_008988	SML0445
Loratadine	Sigma-Aldrich RRID:SCR_008988	L9664

Supplementary table 1 Continued.

Critical commercial assays		
Assay	**Source**	**Identifier**
CellTiter 96® AQueous One Solution Cell Proliferation Assay	Promega RRID:SCR_006724	G3581
RealTime-Glo™ Annexin V Apoptosis and Necrosis Assay	Promega RRID:SCR_006724	JA1012
Critical equipment and software		
Assay	**Source**	**Identifier**
Celígo® Imaging Cytometer	Nexcelom Bioscience	-
SpextraMax iD3	MolecularDevices	
Image J version 1.48v	https://imagej.net/	RRID:SCR_003070
Confocal TCS_SP8	Leica Microsystems RRID:SCR_008960	-
Critical equipment and software		
Assay	**Source**	**Identifier**
IVIS Lumina Imaging System	Caliper LifeSciences, USA	-
MIDI slidescanner	Pannoramic	-
Caseviewer	3DHistech	RRID:SCR_017654

► Supplementary figure 1 CADs reduced viability in a panel of human bladder cancer cells.
*Assessment of the viability of T24 (**A**) and RT-112 (**B**) cells after treatment with a dose range of 8 different CADs for 40h. Assessment of the viability of T24 (**C**) and RT-112 (**D**) cells after 4hrs treatment. CADs were replaced by regular growth medium after 4h and 40h later live cell count was quantified in a Celigo(R) cytometer as the total cell count (Hoechst-positive cells) - dead cell count (Propidium Iodide-positive cells). Mean +/- SE normalized to vehicle treated cells. One-way ANOVA *p<0.05; **p<0.01; ***p<0.001 Multiple subconfluent UCB cells were treated for 2h with a dose range of either astemizole (**E**), terfenadine (**F**) or penfluridol (**G**). Viability was measured using MTT assay after 48h. Mean +/- SE normalized to respective vehicle treated UCB cells. (**H**) Confluent UM-UC-3 cells were treated for 2h with a dose range of penfluridol. Viability was measured using MTT assay after 48h. Mean +/- SE normalized to vehicle treated cells. (n=3; 6 replicates each). One-way ANOVA *p<0.05; **p<0.01; ***p<0.001.*

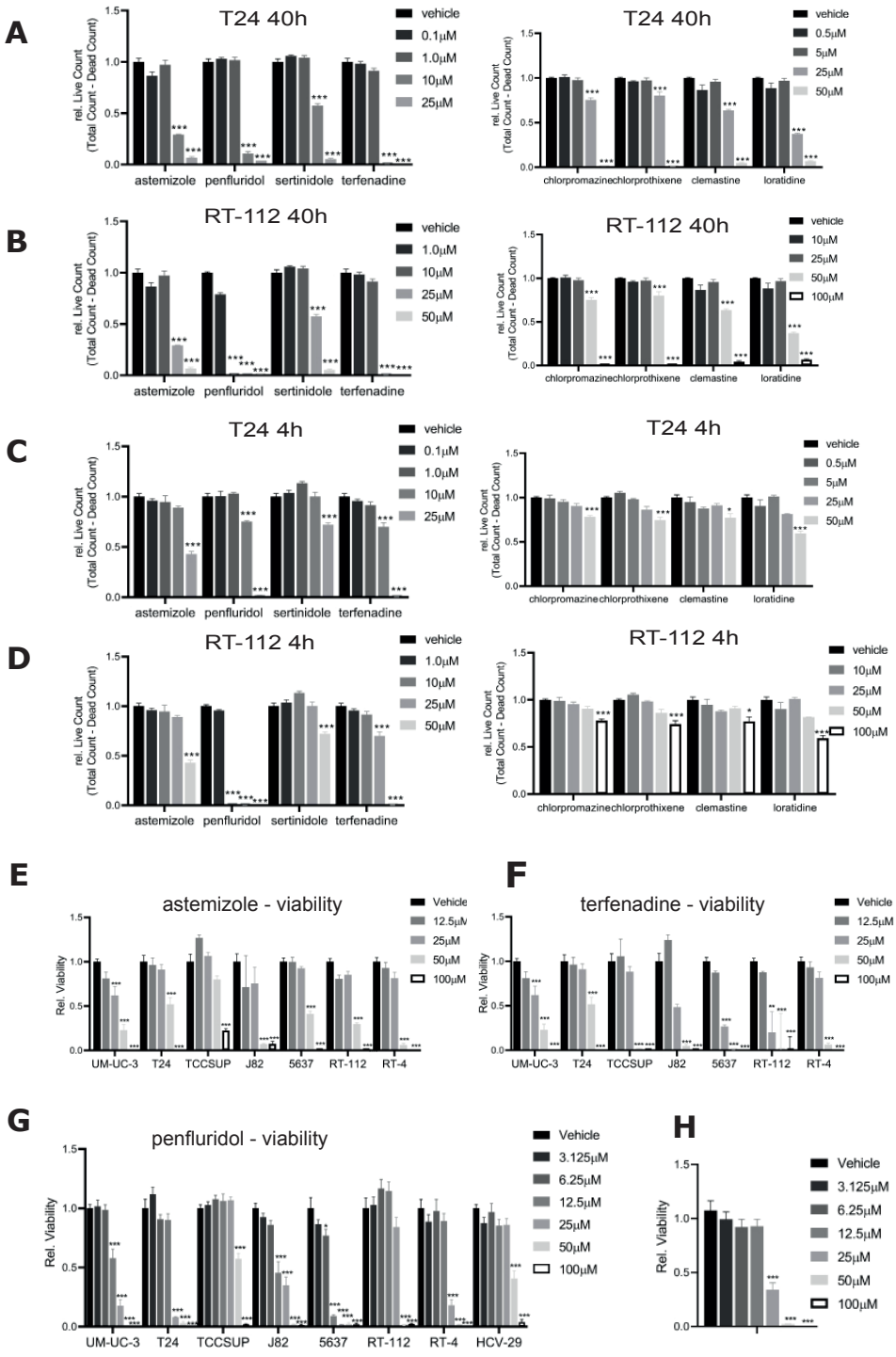
A
T24 40h
rel. Live Count (Total Count - Dead Count)
vehicle
0.1μM
1.0μM
10μM
25μM
astemizole
penfluridol
sertinidole
terfenadine
T24 40h
vehicle
0.5μM
5μM
25μM
50μM
chlorpromazine
chlorprothixene
clemastine
loratidine
B
RT-112 40h
vehicle
1.0μM
10μM
25μM
50μM
RT-112 40h
vehicle
10μM
25μM
50μM
100μM
C
T24 4h
vehicle
0.1μM
1.0μM
10μM
25μM
T24 4h
vehicle
0.5μM
5μM
25μM
50μM
D
RT-112 4h
vehicle
1.0μM
10μM
25μM
50μM
RT-112 4h
vehicle
10μM
25μM
50μM
100μM
E
astemizole - viability
Rel. Viability
Vehicle
12.5μM
25μM
50μM
100μM
UM-UC-3
T24
TCCSUP
J82
5637
RT-112
RT-4
F
terfenadine - viability
G
penfluridol - viability
Vehicle
3.125μM
6.25μM
12.5μM
25μM
50μM
100μM
HCV-29
H

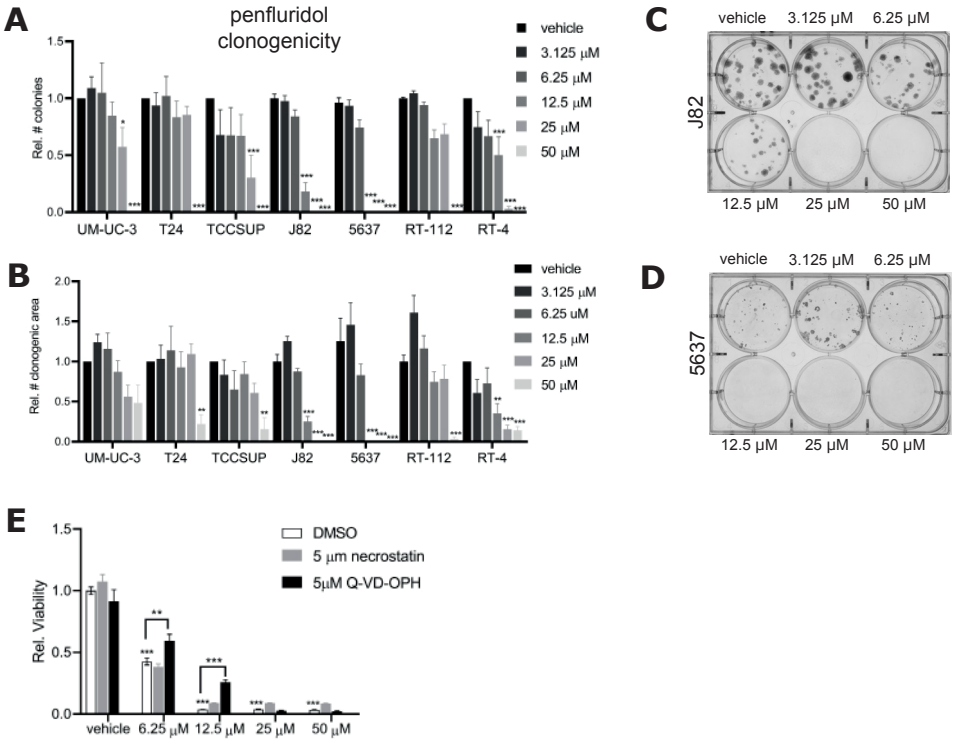

Supplementary figure 2 CADs reduced viability and clonogenicity in a panel of human bladder cancer cells.

*Clonogenic assay: multiple bladder cancer cells were treated for 2h with a dose range of penfluridol and subsequently after 10-14 days, (**A**) number of colonies and (**B**) clonogenic area were measured using Image J. Representative images of clonogenic assay of respectively J82 (**C**) and 5637 (**D**) cells. (n=3; 3 replicates each). One-Way ANOVA. *p<0.05; **p<0.01; ***p<0.001. (**E**) Mitochondrial activity was measured after 24h in response to treatment with a dose range of penfluridol in combination with either necroptosis inhibitor NS1 or pan-caspase inhibitor Q-VD-OPh. Mean+/- SE normalized to vehicle treated UM-UC-3 cells (n=3; 6 replicates each). One-way ANOVA. *p<0.05; **p<0.01; ***p<0.001.*

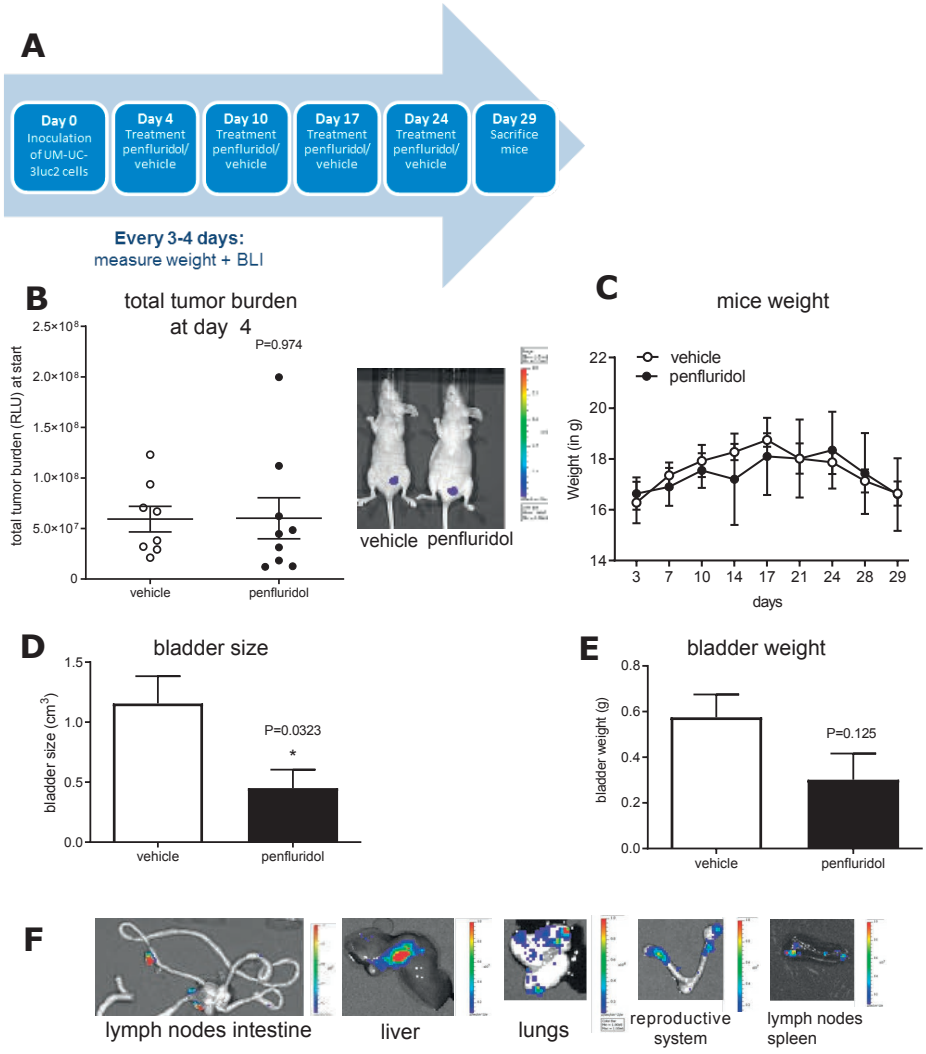

Supplementary figure 3 Anti-tumor effects of penfluridol in an orthotopic murine xenograft model with stable firefly luciferase-2 UM-UC-3 human bladder cancer cells.

*Female BALB/C nu/nu mice were inoculated with UM-UC-3 luciferase 2 bladder cancer cells and intravesically treated with vehicle (n=8) or penfluridol (n=9; 100 µM once weekly; equivalent to 130 µg/kg/w). (**A**) Schematic overview of the experiment. (**B**) Mice were divided into 2 groups with equal tumor burden based on total tumor burden; representative BLI images of mice are shown. (**C**) Weight of the mice over time. (**D**) Bladder size in cm3 at day 29. (**E**) Bladder weight in g at day 29. (**F**) Representative BLI images of metastasis in intestinal lymph nodes, liver, spleen, reproductive system, and lungs at day 29. Mann-Whitney-U test. *p<0.05; **p<0.01; ***p<0.001.*

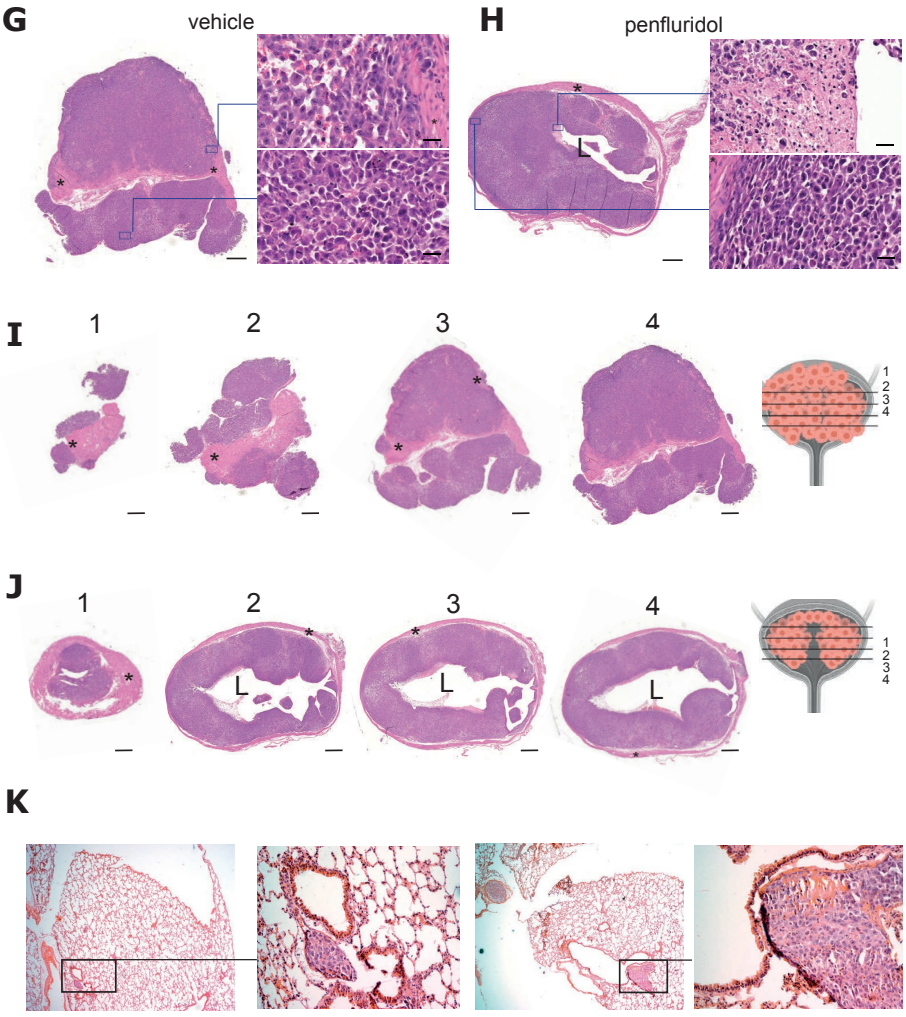

Supplementary figure 3 Anti-tumor effects of penfluridol in an orthotopic murine xenograft model with stable firefly luciferase-2 UM-UC-3 human bladder cancer cells.

*Representative images of vehicle (**G**) and penfluridol (**H**) treated bladders stained with Hematoxylin & Eosin with respective magnifications. Scale bar 500 and 20 µm respectively. (**I**) Representative images of vehicle treated bladders stained with Hematoxylin & Eosin at different planes of sectioning displaying muscle-invasion. Scale bar 500 µm. Schematic overview of the bladders is shown next to the different planes (created with Biorender.com).(**J**) Representative images of penfluridol treated bladders stained with Hematoxylin & Eosin at different planes of sectioning. Scale bar 500 µm. (**K**) Representative Hematoxylin & Eosin images of a metastasis in a lung. L: lumen; * muscle layer.*

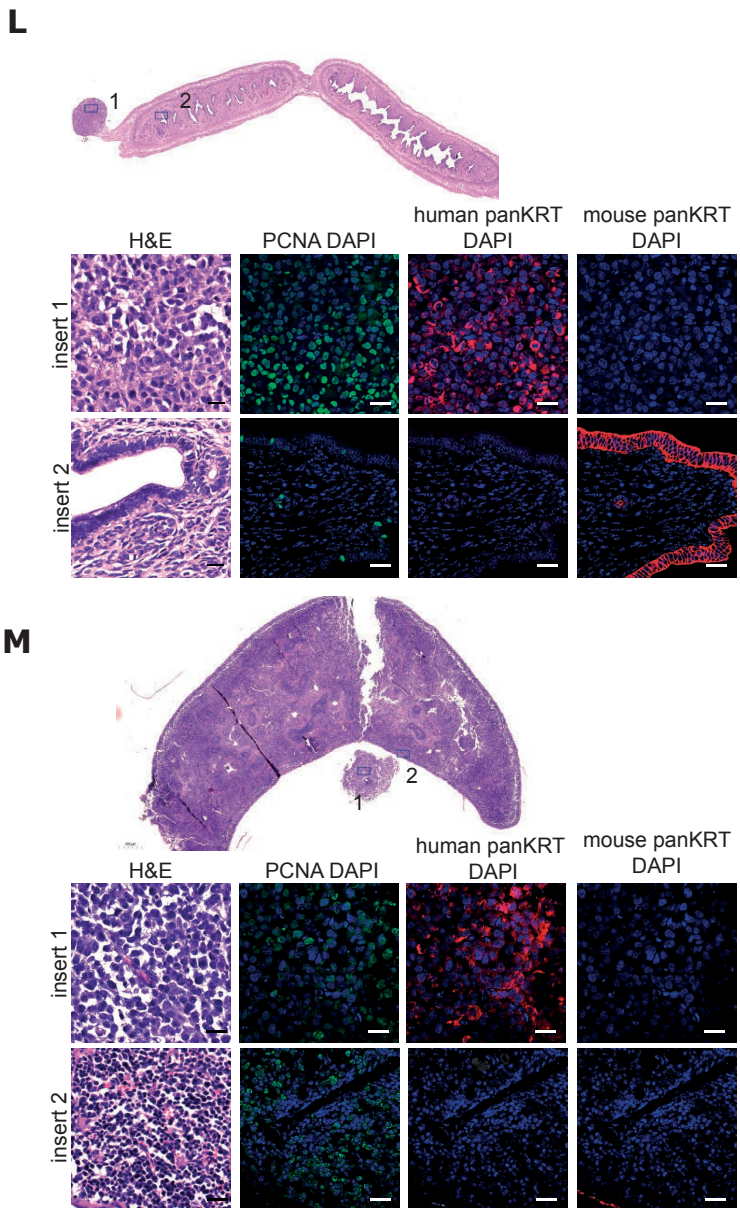

Supplementary figure 3 Anti-tumor effects of penfluridol in an orthotopic murine xenograft model with stable firefly luciferase-2 UM-UC-3 human bladder cancer cells.

*(**L**) Representative image of a metastasis in a lymph node (adjacent to spleen). (**M**) Representative image of a metastasis in the reproductive system. Scale bar for overview 500mm. PCNA: green, panKRT (human or mouse): red and DAPI blue. Scalebar 25 µm.*

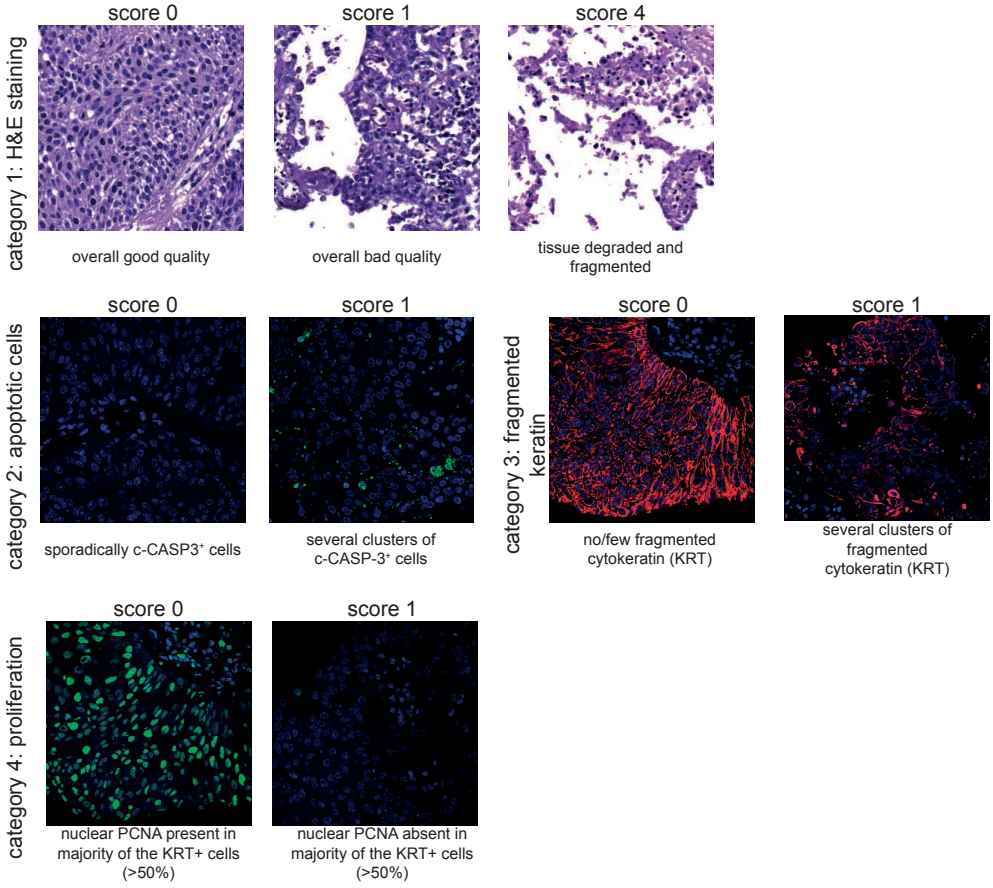

Supplementary figure 4 Scoring of ex-vivo cultured human bladder cancer slices.

Multiple explanted tissue slices were cultured for each condition. Cumulative score is based on histological evaluation of entire tissue slice. Representative images are shown. First, overall quality of the TS was scored based on H&E staining (category 1). TS received a score of either 0, 1 or 4. TS received a score of 1 when overall quality was poor in >50% of the H&E stained TS. The TS scored the maximum score of 4 when tissue was completely degraded or fragmented. When TS did not already directly receive a score of 4 for overall quality based on the H&E stained tissue, sections were subsequently scored for 3 additional categories: 2) presence of cleaved-caspase 3+(c-CASP-3+)/Keratin+ (KRT+) cells, 3) fragmented KRT, and 4) nuclear proliferation based on proliferation cell nuclear antigen (PCNA). TS received a score of either 0 or 1 for each category. For category 2 and 3, TS received a score of 1 when multiple clusters were observed. For category 4, TS received a score of 1 when <50% of KRT+ cells in the TS displayed nuclear PCNA. Cumulative score was calculated as the sum of the 4 categories, median cumulative scores are shown. c-CASP-3 and PCNA: green, panKRT red and DAPI blue.

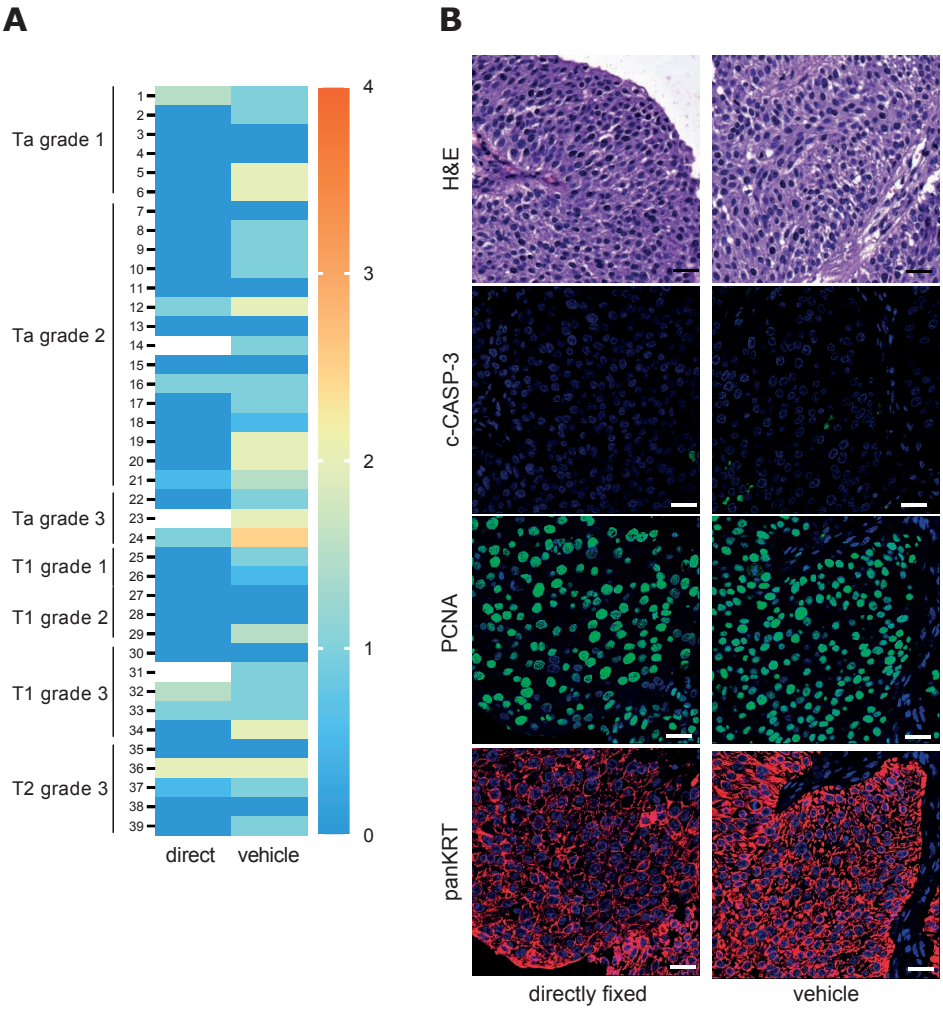

Supplementary figure 5 Ex-vivo treatment of cultured human bladder cancer slices with penfluridol: directly fixed vs cultured tissue.

*(**A**) heat map showing the median scores of the bladder cancer slices per patient (sum of the scores based on PCNA, c-CASP-3, fragmented KRT and H&E staining). Bladder cancer slices from directly fixed and ex vivo cultured in vehicle solution for 3 days. (**B**) representative images of bladder cancer tissue obtained from a patient diagnosed with NMIBC stage T1 grade 2 (#28) directly fixed or cultured for 3 days in the presence of vehicle solution. c-CASP-3 and PCNA: green, panKRT red and DAPI blue. Scalebar 25 µm.*

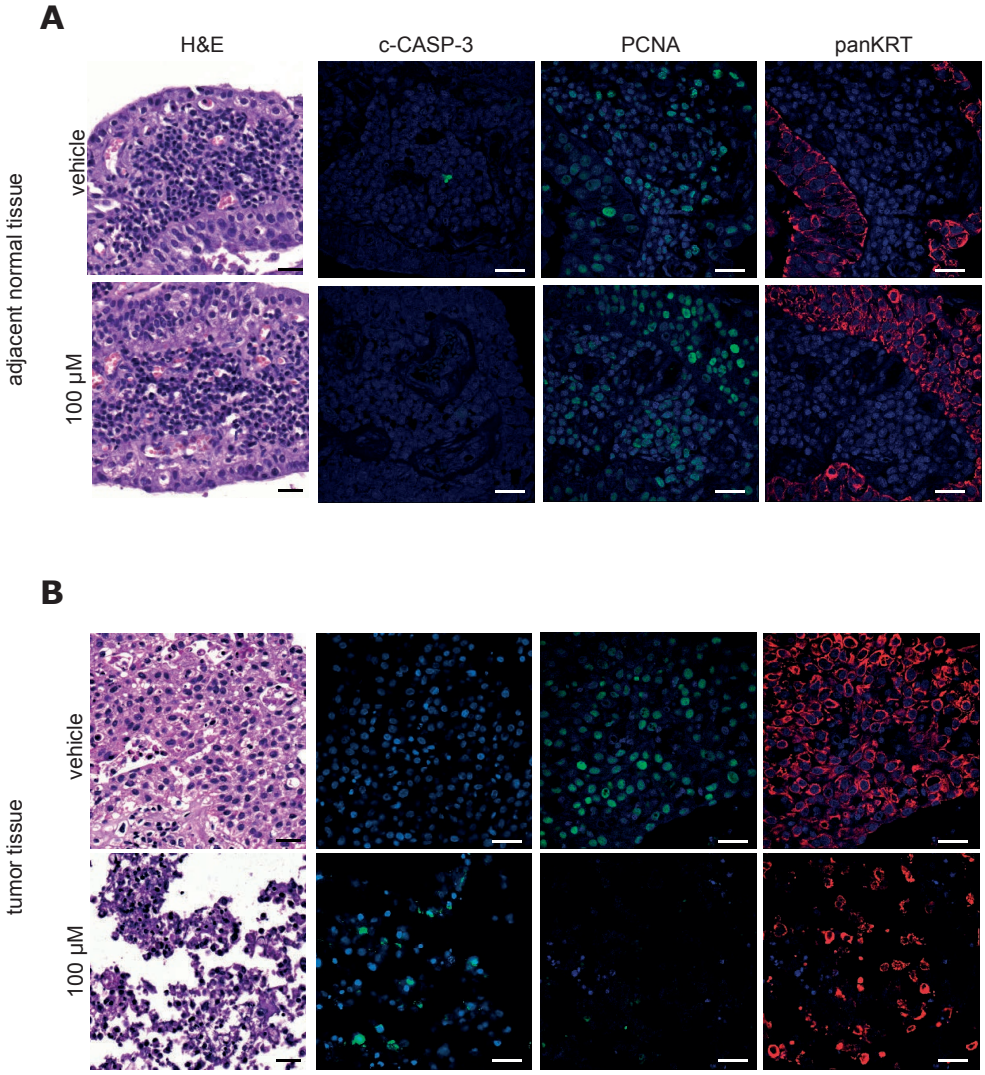

Supplementary figure 6 Evaluation of the effect of penfluridol on normal human urothelium. *(**A**) Representative images of urothelium in tissue slices obtained from adjacent normal tissue from a bladder cancer patient with NMIBC T1 grade 2 (#29). (**B**) Representative images of tissue slices from tumor tissue from this patient (#29). H&E, c-CASP-3 and PCNA: green, panKRT red and DAPI blue. Scalebar 25 µm.*

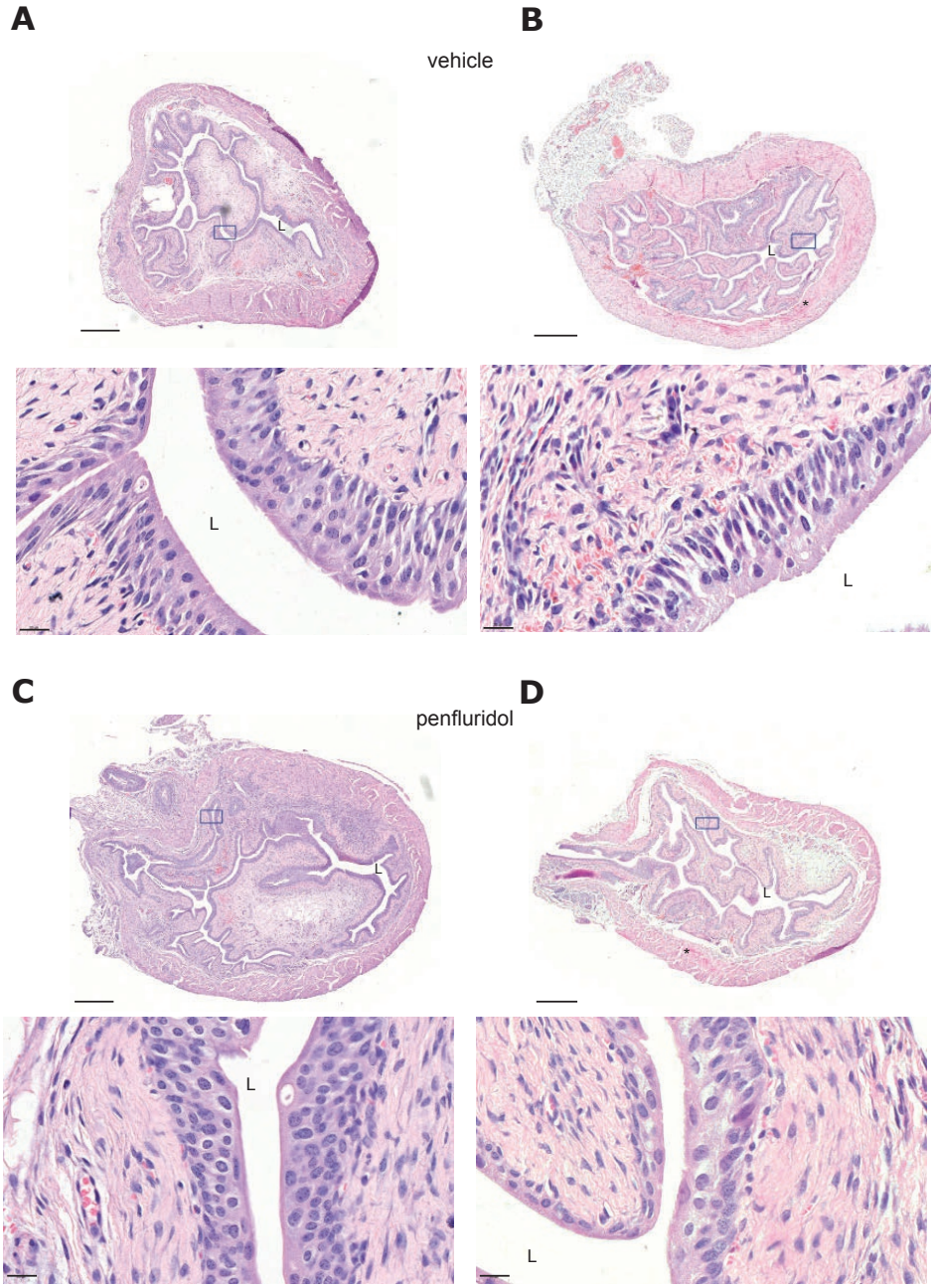

Supplementary Figure 7 Evaluation of the effect of penfluridol on normal murine urothelium.
*(**A**) Representative overview images of H&E stained non-tumor bearing murine bladders of vehicle-treated (**A-B**) and 100 µM penfluridol-treated (**C-D**) mice. L: lumen; * muscle layer*

Supplementary information

Cationic Amphiphilic Drugs
Penfluridol, astemizole and terfenadine were obtained from Sigma-Aldrich®. Penfluridol (P3371) and terfenadine (T9652) were diluted in Absolute EtOH (EMSURE®) to a stock solution of 50 mM. Likewise, astemizole (A2861), sertinidole (S8072), chlorprothixene (C1671), chlorpotmazine (C8138), clemastine (SML0445) and loratadine (L9664) were diluted in dimethyl sulfoxide (DMSO; Sigma-Aldrich®) to a stock solution of 50 mM (**Supplementary table 2**). Serial dilutions were established by diluting these stock solutions in the cell-specific medium of the various cell lines (**Supplementary table 1**).

In vitro Viability assay
Cells were seeded in a 96-wells plate at a concentration of 1500 single cells per well with 6 technical replicates. Cells were either treated after 24h, or cells were allowed to grow until confluency and subsequently treated for 2h with a dose range. After replacing the medium, cells were incubated at 37°C for an additional 24, 48 or 72h. Subsequently, 20µl of MTS reagent was added and after 2 hours, the OD was measured at 490nm using the VersaMax ELISA Microplate Reader. Apoptotic nuclear condensation was evaluated in Hoechst-33342 stained cells using Olympus IX81 microscope with a 20 × Olympus objective, Scan^R automated acquisition software (version 2.3.0.5) and analysis with ImageJ (version 1.48v).

In vitro clonogenicity
100-single cells were seeded in a 6-wells plate. After 24h, cells were treated with a dose-range of penfluridol for 2h. After replacing medium, cells were incubated at 37°C. After ~14 days, cells were fixed with 4%PFA and stained for 10 minutes with 5% crystal-violet. The number of colonies and colony area were calculated with ImageJ software.

In vitro Lysosomal membrane permeabilization
60000 cells were seeded on PET-coated chamber slides and left for 24h to adhere. Cells were treated with a dose-range of penfluridol for 2h. After 24h lysosomal membrane permeabilization was detected by staining paraformaldehyde-fixed cells with LGALS1 and LAMP-1 primary antibodies (**Supplementary table 1**) at 4°C. DAPI staining was used to visualized the nuclei. Next, the slides were stained for 1.5h at RT with DαM 488 secondary antibody and mounted with prolong Gold antifade. Confocal images were taken with the Confocal TCS_SP8 (Leica).

Near-patient ex vivo bladder cancer cultures
Tumor tissues from patients diagnosed with various stages of UCB were obtained during transurethral resection of the bladder upon informed consent (MEC-2014-553). Explanted tumor tissue slices (TS) were sectioned and cultured as previously described (20, 21). Bladder cancer material was transported in EMEM medium at RT, transferred into Penicillin Streptomycin solution for 10 minutes and cut into consecutive tissue slices of approximately 500-1000 µm thick (20). The tissues slices were placed on nitrocellulose filter inserts (6 well filter inserts, pore size of 3 µm, Corning Costar) and cultured with EMEM, supplemented with 10% FCS and 1% Pen-Strep. The tissue was cultured in an oxygenated and sealed system. After 24 hours, the tissue slices were treated with either vehicle solution or penfluridol (depending on the amount of tissue either 100µM or a dose range). At 3 days post treatment, the tissue was fixed in 4% PFA for 1 hour at RT and transferred into a plastic cassette and stored in 70% ethanol at 4°C prior to paraffin embedding.

Histology
Haematoxylin and eosin staining (H&E) was performed according to a standard protocol to assess general histology. For immunofluorescence staining, deparaffinization was performed via incubation in Histoclear (National Diagnostics, HS-200) and rehydrated by incubation in a series of decreasing concentrations of ethanol. Antigen retrieval was performed by cooking the slides in unmasking solution (Vector Labs, H-3300) in the pressure cooker. After blocking with 1% BSA (Sigma-Aldrich, A7906) for 30 minutes, the slides were incubated overnight with primary antibody at 4°C. Next, the slides were stained for 1.5 hours at RT with secondary antibody and mounted with prolong Gold antifade (Molecular probes, Thermofisher Scientific, P36930) (**Supplementary table 1**).

Orthotopic inoculation tumour cells
-Anaesthetize mouse with isoflurane (see below), induce miction by administering mild abdominal pressure.
-Administer Temgesic according protocol. (see below)
-Place the mouse ventrally on a cardboard piece
-Tape the tail to the cardboard
- Remove the catheter (Jelco I.V. Catheter Radiopaque 24G, ¾G, Smiths medical ref 4053) from the needle and put some instilla gel (Farco-PHARMA GmbH Koln, Germany) on the catheter.
- Hold the urethra with a pair of tweezers and gently insert the catheter into the urethra. If you feel some resistance, pull back and try a different angle. The catheter should enter the urethra easily.

- Insert 1 cm of the catheter and tape the catheter on top of the tail.
- Rinse the bladder with 1 ml PBS (Check if the liquid has been equilibrated to room or body temperature)
-Fill a syringe with HCl (0.1M)and place the needle on it. Inject approx. 100 ul into the bladder
- Stir, using a back and forth motion of the syringe for 15" (1 stroke/sec) and remove the HCl.
- Inject 100 ul KOH (0.1M) to neutralize the HCl.
- Stir, using a back and forth motion of the syringe for 15" (1 stroke/sec) and remove the KOH
- Inject cell suspension (5*10^6 in 35 µl PBS)
- Close the urethra by binding it off using a suture (Prolene Ethicon 6-0 13mm 3/8c). Let someone remove the catheter while binding off.
- Remove tape
- Keep the mouse anaesthetized with his lower body lifted slightly up for 2 hours
- Cut suture open before ending the anaesthesia.

Administration of Analgesia (Temgesic)
- Prepare temgesic solution (dosage: 0.1 mg/kg buprenorphine s.c. every 8 hours as needed)
- Check if the liquid has been equilibrated to room or body temperature.
- Fill the syringe with the substance that needs to be injected. Make sure there are no air bubbles in the syringe and that the needle is filled with fluid.
- Take the animal from out of the cage.
- Hold the scruff of the animal between thumb and forefinger and restrain the tail.
- Disinfect the injection place with a cotton swab wetted with ethanol 70%.
- Carefully insert the needle, between thumb and forefinger and into the center of the triangular shaped section of the scruff. Keep the needle and syringe parallel to the mouse's head and back.
- Carefully and slowly insert the substance by pushing down the plunger. You can feel the bulging of the substance between your fingers.
- Carefully remove the needle from the scruff of the animal.
- Check the injection site for liquid flowing back or blood loss. Do not return the mouse to its cage unless the injection site is clean and dry. - Place the animal back into the cage. Assure yourself of the proper/ normal movement of the animal
- Check your animal for signs of pain or discomfort at least 6-8 hours after initial dose to determine if there is the need for additional analgesia

Intravesical Instillation
- Anaesthesize mouse with isoflurane (see below)
- Administer Temgesic according to protocol. (see below)
- Place the mouse ventrally on a cardboard piece
- Remove the catheter (Jelco I.V. Catheter Radiopaque 24G, ¾G, Smiths medical ref 4053) from the needle and put some instilla gel (Farco-PHARMA GmbH Koln, Germany) on the catheter.
- Prior to the rinsing, the bladder will be emptied by mild abdominal massage, to induce a better contact between compound and urothelial cells.
- Hold the urethra with a pair of tweezers and gently insert the catheter into the urethra. If you feel some resistance, pull back and try a different angle. The catheter should enter the urethra easily.
- Insert 1 cm of the catheter and tape the catheter on top of the tail.
- Rinse the bladder with 1 ml PBS (Check if the liquid has been equilibrated to room or body temperature)
- Tie a suture around the urethra, but do not pull tight yet.
- Insert the needle and inject 50 µl of the compound.
- Tighten the suture, while a second person, first removes the needle. Directly followed by the catheter.
- During 1 hour, the mice are regularly turned to contact the whole bladder surface with the compound.
- After 1 hours the suture will be removed and the bladder will be emptied by mild abdominal compression.
- Mice will be daily checked for weight, behavioural changes and blood in urine.

Anaesthesia
- Isoflurane: induction phase: 2 – 4 %, maintenance phase: 0.25 – 2%
- Airflow: induction phase: 0.8 L/min, maintenance phase: 0.4 L/min
- When operation takes longer than 15 min. the airflow (from DL meter) needs to be enriched with O2 till 30-40%.

Bioluminescence measurements
Outgrowth of spread of the tumour cells was monitored (number of measurements depending on the experiment) by whole body bioluminescent imaging (BLI) using an intensified charge-coupled device (CCD) video camera in a light-tight specimen box of the *in vivo* Imaging System (IVIS Lumina). Animals were anesthetized with isoflurane and were given D-luciferin (15 mg/ml in D-PBS; 25 µl/10 g body weight) by intraperitoneal injection. Mice were placed into the light-tight camera box with continuous exposure to isoflurane. Imaging time ranged from 10 s to

1 min (generally 30s), depending on the tumor model, 5 min after D-luciferin injection. Three mice were imaged each time from a dorsal and a ventral view. The photons emitted from the bioluminescent tumours or cells were detected by the IVIS camera system, integrated, digitized and displayed. When saturated pictures are taken, first the F-stop is adjusted (diaphragm). If the image is still saturated, the image time can be adjusted.

Intraperitoneal injections (luciferin)
- Check if the liquid has been equilibrated to room or body temperature.
- Fill the syringe with the substance that needs to be injected. Make sure that there are no air bubbles in the syringe and that the needle is filled with fluid.
- Take the animal from out the cage
- Restrain the animal. Hold the animal with the belly facing up, tilting the animal in a head down position.
- Disinfect the injection place with a gauze wetted with ethanol 70%.
- Insert the needle, with the bevel facing up, into the animal's lower right abdominal quadrant, avoiding the abdominal midline so that you will not inject into the urinary bladder
- Carefully retract the plunger to check if you haven't hit a blood vessel
- With no blood in the syringe gently inject the substance.
- Carefully remove the needle from the animal
- Check the injection site for liquid flowing back or blood loss.
- Place the animal back into the cage. Check for proper/ normal movement of the animal.

Cervical dislocation
- Anaesthetize the mouse with isoflurane.
- Place the thumb and first finger of the other hand against the back of the neck at the base of the skull
- To produce the dislocation, quickly push forward and downward with the hand or object restraining the head, while pulling backward with the hand holding the tail base
- The effectiveness of dislocation can be verified by feeling for a separation of cervical tissues. When the spinal cord is severed, a 2-4 mm space will be palpable between the occipital condyles and the first cervical vertebra. Occasionally, however, the dislocation occurs between thoracic vertebrae. Check closely to confirm respiratory arrest and when possible, verify by palpation, that there is no heart beat.

Quantification of signals

Quantification of signals was performed by the Living Image® (Xenogen) software. Values were expressed as RLUs in photons/second. Numbers of metastases per animal were counted by eye from a dorsal and ventral view.